European Journal of Medicinal Chemistry 154 (2018) 9–28

Contents lists available at ScienceDirect

European Journal of Medicinal Chemistry

journal homepage: http://www.elsevier.com/locate/ejmech

Research paper

Design, synthesis and biological evaluation of a series of novel 2-benzamide-4-(6-oxy-N-methyl-1-naphthamide)-pyridine derivatives as potent fibroblast growth factor receptor (FGFR) inhibitors

Manman Wei [a, d, 1], Xia Peng [b, d, 1], Li Xing [a], Yang Dai [b, d], Ruimin Huang [c, d], Meiyu Geng [b, d], Ao Zhang [a, c, d], Jing Ai [b, d, **], Zilan Song [a, d, *]

[a] CAS Key Laboratory of Receptor Research and the State Key Laboratory for Drug Research, Shanghai Institute of Materia Medica (SIMM), Chinese Academy of Sciences, Shanghai, 201203, China
[b] Division of Anti-tumor Pharmacology, State Key Laboratory of Drug Research, Shanghai Institute of Materia Medica (SIMM), Chinese Academy of Sciences, Shanghai, 201203, China
[c] School of Life Science and Technology, ShanghaiTech University, Shanghai, 200031, China
[d] University of Chinese Academy of Sciences, 19A Yuquan Road, Beijing, 100049, China

ARTICLE INFO

Article history:
Received 5 March 2018
Received in revised form
8 April 2018
Accepted 4 May 2018

Keywords:
FGFR
VEGFR
Synergistic effect
Tumor growth inhibition
Lucitanib

ABSTRACT

Starting from the phase II clinical FGFR inhibitor lucitanib (**2**), we conducted a medicinal chemistry approach by opening the central quinoline skeleton coupled with a scaffold hopping process thus leading to a series of novel 2-benzamide-4-(6-oxy-N-methyl-1-naphthamide)-pyridine derivatives. Compound **25a** was identified to show selective and equally high potency against FGFR1/2 and VEGFR2 with IC_{50} values less than 5.0 nM. Significant antiproliferative effects on both FGFR1/2 and VEGFR2 aberrant cancer cells were observed. In the SNU-16 xenograft model, compound **25a** showed tumor growth inhibition rates of 25.0% and 81.0% at doses of 10 mg/kg and 50 mg/kg, respectively, with 5% and 10%body weight loss. In view of the synergistic potential of FGFs and VEGFs in tumor angiogenesis observed in preclinical studies, the FGFR/VEGFR2 dual inhibitor **25a** may achieve better clinical benefits.

1. Introduction

The fibroblast growth factor receptors (FGFRs) are a family of highly conserved transmembrane tyrosine kinases (RTKs), which constitute four members (FGFR1-4) [1–4]. The FGF-FGFR axis is involved in signal transduction pathways that regulate cell proliferation, differentiation, embryonic development, migration, survival, angiogenesis and organogenesis [3,5–8]. Over the past decades, several genomic alterations in the FGF-FGFR axis including activation mutations, gene amplifications, and chromosomal translocations have been identified in a broad spectrum of human tumors as oncogenic drivers, thus offering a new strategy to develop molecular targeted personalized medicine based on the FGFR activation status in cancer patients [9–15]. Since FGFR, like other RTKs (EGFR, VEGFR2), shares a ubiquitous intracellular signaling pathway, cancer cells are prone to escape the FGFR inhibition by either genomic mutations or by shifting to parallel signaling pathways [16–20]. Accordingly, the currently approved FGFR inhibitors are multi-target inhibitors (e.g. lenvatinib [21], nintedanib [22], pazopanib [23]) exerting antitumor efficacy primarily through targeting other RTKs rather than FGFRs [8]. Therefore, there is a need to develop more selective inhibitors to suppress tumors clearly through targeting FGFRs by using FGFR activation status as a biomarker to stratify patients [24,25]. To this end, several FGFR-selective inhibitors, including AZD4547 (**1**) [26] and BGJ398 (**3**) [27] (Fig. 1) have been in extensive clinic trials, and the outcome of these investigations will be useful to validate FGFR inhibitors as single anticancer therapies [28,29]. On the other hand, it is known that tumor angiogenesis is augmented by cross-talking between

* Corresponding author. CAS Key Laboratory of Receptor Research and the State Key Laboratory for Drug Research, Shanghai Institute of *Materia Medica* (SIMM), Chinese Academy of Sciences, Shanghai, 201203, China
** Corresponding author. Division of Anti-tumor Pharmacology, State Key Laboratory of Drug Research, Shanghai Institute of *Materia Medica* (SIMM), Chinese Academy of Sciences, Shanghai, 201203, China.
E-mail addresses: jai@simm.ac.cn (J. Ai), songalan@simm.ac.cn (Z. Song).
[1] These two authors contributed to this work equally.

https://doi.org/10.1016/j.ejmech.2018.05.005
0223-5234/

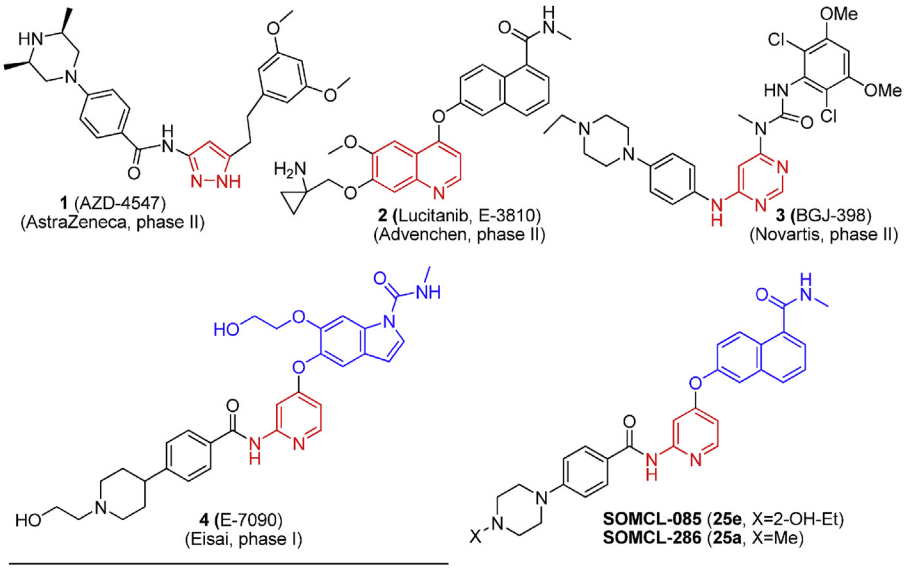

Fig. 1. Representative FGFR inhibitors.

FGF ligands, VEGFRs, and inflammatory mediators in tumor stroma, and the synergistic effects of FGFs and VEGFs in tumor angiogenesis have been observed in preclinical studies [16,30–32]. Therefore, compared to the previous multi-target FGFR inhibitors with less potency against FGFR, development of selective FGFR/VEGFR2 dual inhibitors with equal or even greater potency against FGFR would be an appealing combination [16,17].

The crystal structure of **1** [34] with FGFR1 demonstrates that the 3,5-dimethoxy-phenyl moiety occupies the hydrophobic pocket to form a hydrogen bond with the Asp641 residue. The pyrazole core located in the hinge region forms two hydrogen bonds with the carbonyl of the Glu562 and the NH of the Tyr563 residues. The substituted benzamide extends toward solvent, making two hydrogen bonds with the carbonyl of Ala564 and the NH of Gly485. The binding mode of another non-selective clinically being investigated FGFR inhibitor lucitanib (**2**) [33,34] with FGFR1 is similar to that of **1**. The *N*-methyl-1-naphthamide fragment forms two hydrogen bonds with the carbonyl of the Glu531 and the NH of the Asp641 residues, and extends to the hydrophobic pocket. The quinoline moiety forms a hydrogen bond with the NH of the Ala564 residue in the hinge region.

In view of the similar binding patterns of **1** and **2** with FGFR1, we envisioned that opening the quinoline fragment of **2** and introducing an amide bond as the hydrogen bond acceptor and donor would generate structurally flexible new FGFR inhibitors retaining similar hydrogen bonding networks (Fig. 2). Following this approach, we identified compound **SOMCL-085** [35] (**25e**, Fig. 1) that showed nearly equal potency against FGFR and VEGFR2 (Fig. 2). Encouraged by this result, a series of novel 2-benzamide-4-aryloxypyridine derivatives were developed and a systemic SAR study was conducted leing to the discovery of the preclinical compound **SOMCL-286** (**25a**). Notably, during completion of our study, Eisai disclosed its phase I clinical compound **4** (E−7090) [36], which also bears a 4-aryloxy-2-aminopyridine framework, but with a different head group. This compound showed high potency against FGFR1-3 (0.5–1.2 nM), but weaker potency against VEGFR2 (16 nM), which is different from our FGFR/VEGFR2 dual inhibitor profile. Herein, we report the structure-activity relationship study of our 2-benzamide-4-(6-oxy-N-methyl-1-naphthamide)pyridine series and the pharmacological profiling of the FGFR/VEGFR dual inhibitor **25a**.

2. Chemistry

The synthesis of 2-benzamide-4-aryloxypyridine derivatives is outlined in Schemes 1–5. Nucleophilic displacement of the C-4 fluoro atom of ethyl 4-fluorobenzoates with substituted piperazines afforded compounds **6a-i** in 68–89% yields. Similarly, nucleophilic displacement of the C-2 bromo groups of ethyl 2-bromothiazole-4-carboxylate (**8a**) and ethyl 2-bromooxazole-4-carboxylate (**8b**) and the C-2 chloro group of methyl 2-chloropyrimidine-5-carboxylate (**11**) afforded **9a**, **9b** and **12** in 70–82% yields, respectively. Hydrolysis of **6a-i, 9a, 9b** and **12** afforded the corresponding acids, which were then transformed to acyl chlorides by treating with thionyl chloride and subsequently reacted with ammonium hydroxide to afford primary amide intermediates **7a-i, 10a**, **10b and 13** in 33–70% yields (Scheme 1).

Condensation of 6-(2-chloropyridin-4-yloxy)-1-naphthoic acid (**14**) [37] with CH_3NH_2 afforded intermediate **15** in 96% yield. Compounds **19a-d** were prepared by Buchwald-Hartwig cross-coupling of **15** with benzamides **7a-d** followed by deprotection with CF_3COOH in 49–58% yields for two steps. Treatment of (2-bromoethoxy) (*tert*-butyl)diphenylsilane with 1H-pyrazole-4-carboxamide afforded intermediate **18**, which was converted to compound **20** via cross-coupling with **15** followed by deprotection with CsF in 17% overall yield. Compounds **21a-b** were obtained by cross-coupling of **15** with **10a-b** in 69% and 55% yield, respectively. Similarly, cross-coupling of **15** with **13** followed by deprotection with CF_3COOH afforded compound **22** in 51% yield for two steps (Scheme 2).

Condensation of 6-(2-chloropyridin-4-yloxy)-1-naphthoic acid (**14**) with MeOH afforded **23a** in 95% yield. 2-Chloro-4-(6-oxy-substituted)-pyridine derivatives **23b-e** were synthesized by nucleophilic substitution of 2-chloro-4-nitropyridine with the corresponding phenol derivatives in 40–71% yields. Similarly, nucleophilic displacement of 2,4-dichloropyridine with 2-(3,5-dimethoxyphenyl)ethanol [38] or 2-(2,6-dichloro-3,5-dimethoxyphenyl)ethanol [39] afforded **23f** or **23g** in 71% or 66% yield, respectively. Intermediates **23h-i** were prepared by nucleophilic displacement of 2,6-difluoro-3,5-dimethoxybenzyl methanesulfonate [40] or 1-(3,5-dicholoropyridin- 4-yl)ethyl methanesulfonate [41] with 6-chloropyridin-3-ol in 65% or 61% yield respectively. Compounds **24a-i** were prepared in 52–72%

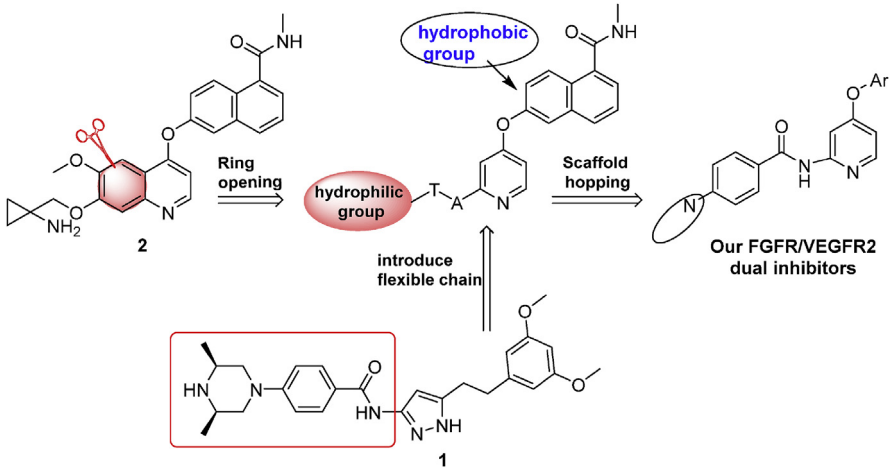

Fig. 2. Design of potent FGFR/VEGFR2 dual inhibitors.

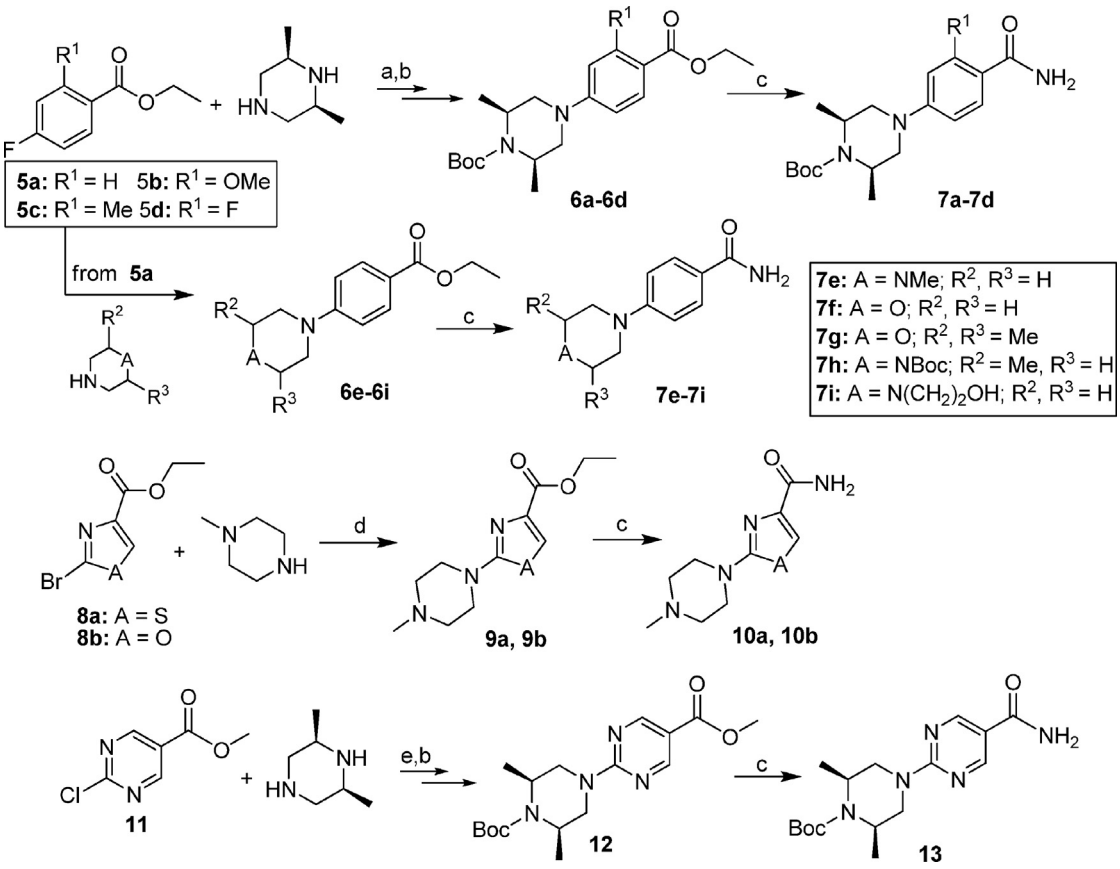

Scheme 1. *Reagents and conditions:* (a) K_2C0_3, DMSO, 110 °C. 75-90%; (b) $(Boc)_2O$, NaOH, DCM/H_2O (1:1), 90-98%; (c) (i) NaOH, MeOH/H_2O (1:1), (ii) $SOCl_2$. DMF, DCM, 0 °C to rt; (iii) NH_4OH, DCM, rt. 33-70%: (d) K_2CO_3. CH_3CN, 80 °C, 70-76%; (e) K_2CO_3, DMF, rt. 75%.

yields by condensation of intermediates **7a** with **23a** or **23b-i** followed by deprotection with CF_3COOH (Scheme 3).

Compounds **25a-e** were prepared via coupling of benzamides **7e-i** with **15** in 49–74% yields. Similarly, reaction of **26** with **15** followed by deprotection with CF_3COOH provided compound **27** in 52% yield, which was then reacted with 2-bromoethanol to afford compound **28** in 62%. Meanwhile, coupling of 4-nitrobenzamide with **15** followed by reduction with zinc powder furnished intermediate **29** in 56% yield, which was then reacted with 1,6-dioxaspiro [2.5]octane or acryloyl chloride to afford compounds **30a,b** in 32% and 80% yield, respectively (Scheme 4).

As shown in Scheme 5, treatment of 4-hydroxy benzamide with 1,2-dibromoethane followed by displacement with different secondary amines furnished intermediates **32a-c** in 31–59% yields, which were then reacted with **15** via cross-coupling to provide compounds **33a-c** in 57–67% yields. Similarly, reaction of ethyl 4-hydroxybenzoate with *tert*-butyl 1-(iodomethyl)cyclopropylcarbamate [43,44] afforded intermediate **31**, which was

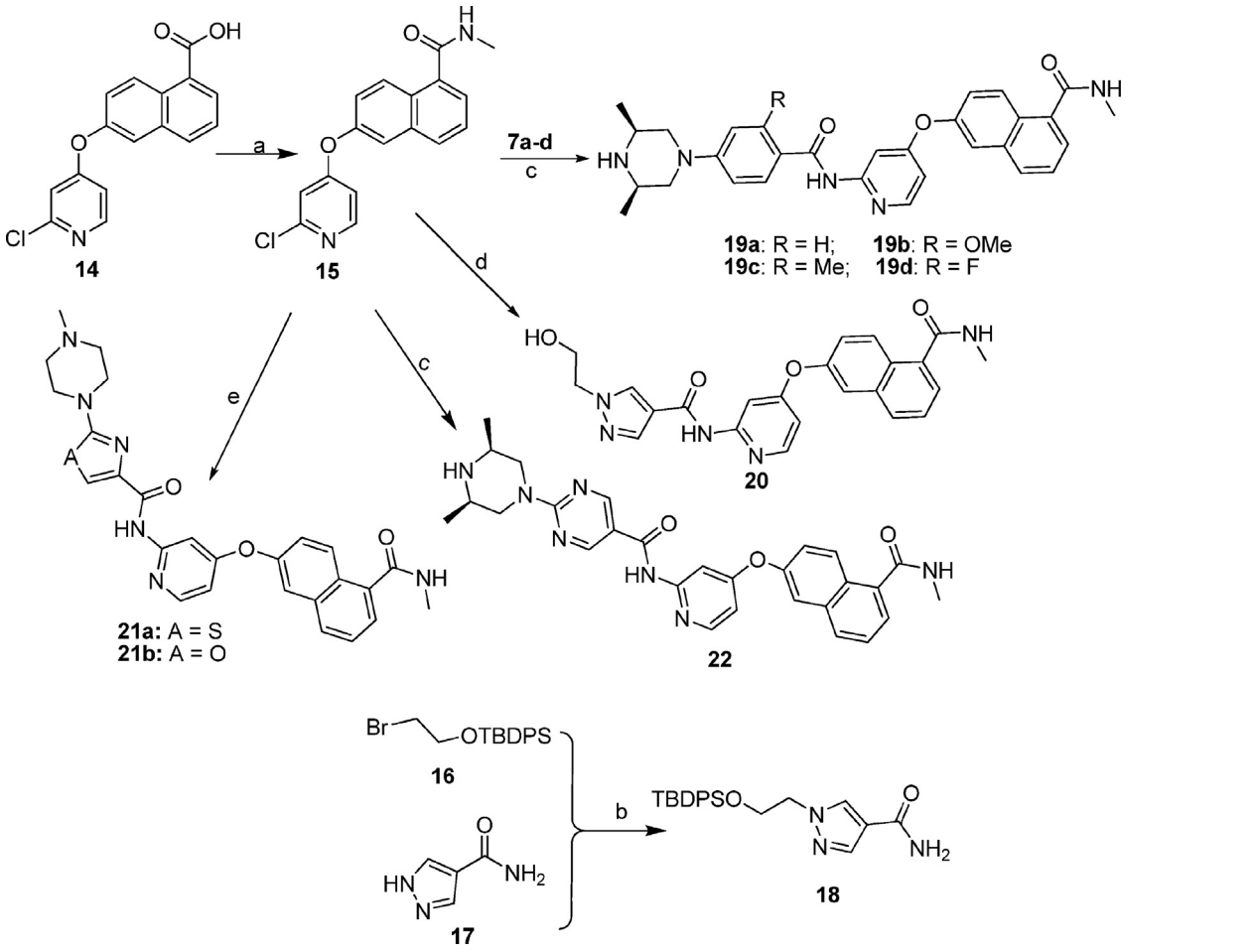

Scheme 2. *Reagents and conditions:* (a) CH_3NH_2, EDCl. HOBt. DIPEA. DCM, rt, 95.8%; (b) K_2CO_3, DMF, 80 °C, 63%; (c) (i) $Pd_2(dba)_3$, Xantpbos, Cs_2CO_3, dioxane, 100 °C; (ii) CF_3COOH. DCM, 49-58% for two steps; (d) **18,** $Pd_2(dba)_3$, Xantphos, CS2CO3, dioxane, 100 °C; (il) CsF, DMF, 80 °C, 27.3% for two steps; (e) **10a-b,** $Pd_2(dba)_3$, Xantpbos, CS_2CO_3, dioxane, 100 °C, 55-69%.

converted to benzamide **32d** in 51% yield in two steps. Subsequent coupling of **32d** with **15** followed by deprotection with CF_3COOH afforded compound **33d** in 55% yield.

3. Results and discussion

3.1. Structure-activity relationships

All the new compounds were assayed for their biochemical activity against FGFR1 and the potent compounds were further tested for their antiproliferative effects in the FGFR1-translocated myeloid leukemia KG-1cancer cells. To test our design, we first incorporated the (3,5-dimethylpiperizin-1-yl)benzamido moiety into the 4-aryloxy-2-aminopyrimidine core as the hydrophilic component leading to compound **19a**. As shown in Table 1, compound **19a** displayed an IC_{50} of 2.1 nM against FGFR1. This compound also displayed high potency of 14.9 nM against the FGFR1-positive KG-1cancer cell. Compared to the phase II clinical FGFR-selective inhibitor **1**, both biochemical and cellular potency of **19a** was lower, therefore, optimization of compound **19a** is needed.

We first focused on optimization of the hydrophilic component by replacing the phenylpiperazine moiety with different substituents. Compounds **19b** and **19c** were obtained by introduction of methoxy and methyl, respectively at the *ortho*-position of the phenyl, both showing reduced potency either in the biochemical (285 vs 12.9 nM) and in the cell (>1 μM) assays. Much worse, the *ortho*-fluorinated compound **19d** nearly completely lost the biochemical activity against FGFR1. Compared to **19a**, both steric and electrostatic effects are likely responsible for the reduced potency of **19b-d**.

Replacement of phenyl in the phenylpiperazine fragment with pyrazole, thiazole, isoxazole, and pyrimidine gave compounds **20**–**22**. All compounds retained good biochemical activity against FGFR1, especially for compounds **21a-b,** both showing IC_{50} values less than 10 nM, however, we failed to obtain their cellular potency due to poor solubility. From the results above, the 4-(3,5-dimethylpiperazin-1-yl)benzamido moiety (as in **19a**) is the best of choice as the hydrophilic component, therefore, it was carried for further optimization.

As shown in Figs. 1 and 2, the hydrophobic pocket in the FGFR1 interaction domain has relatively high tolerance to different heteroaryl rings. Since the *N*-methyl-1-naphthamide fragment as the 4-*O*-substituent of the central pyrimidine in **19a** was initially taken from the clinical compound **2** (lucitanib), we then optimized this component to better fit the hydrophobic pocket by using various heterocyclic bioisosteres or alkyl-aromatic rings as the replacement (Table 2). Compared to compound **19a**, replacing the naphthalene methyl amide with corresponding ester afforded compound **24a** showing slightly reduced biochemical potency (2.1 vs 4.6 nM) but the cellular activity was 10-fold reduced (14.9 vs 159 nM). Adding

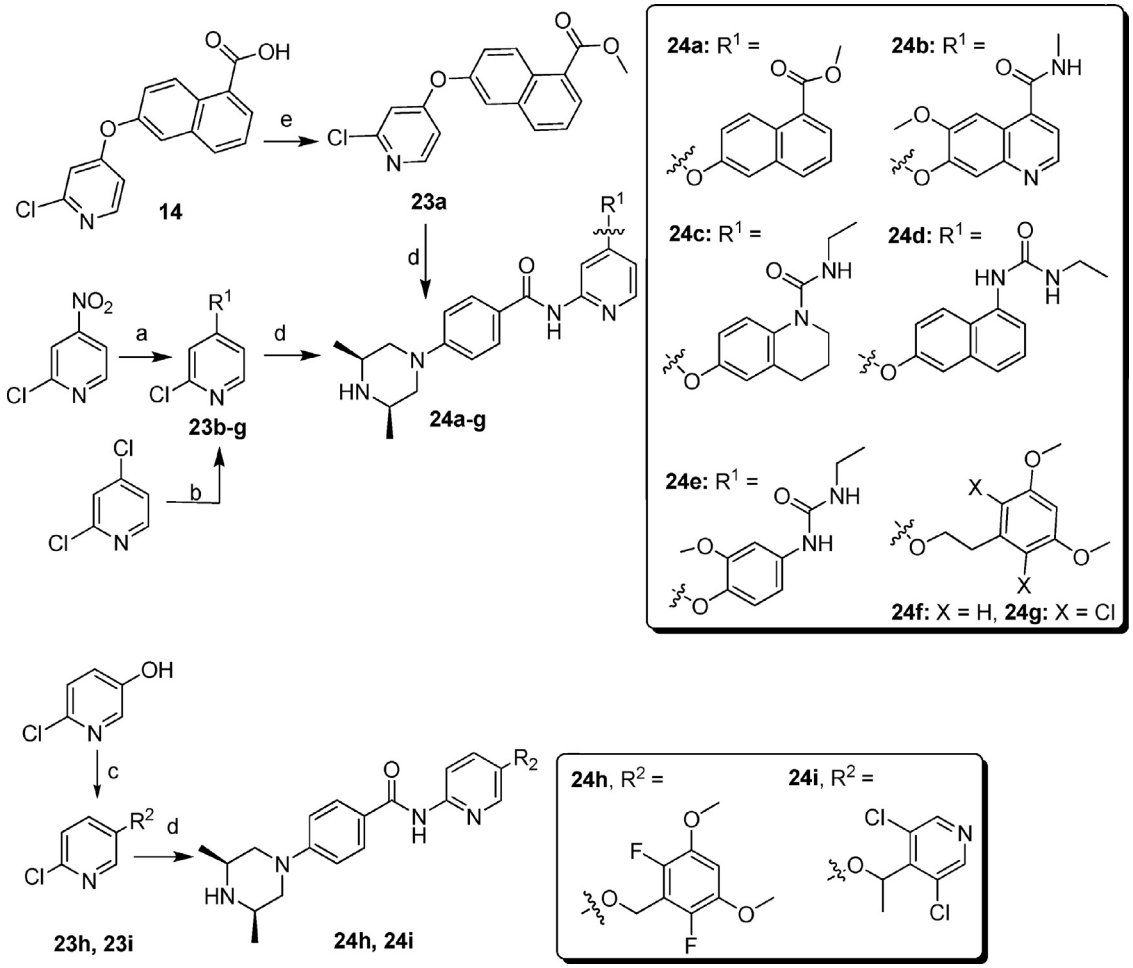

Scheme 3. *Reagents and conditions:* (a) for **23b-e**, phenol derivatives, Cs_2CO_3, DMSO, rt, 40-71%; (b) for **23f**, **23g**, phenylethanol derivatives, t-BuOK, t-BuOH, reflux, 66-71%; (c) methane sulfonates, K_2CO_3. DMF, 60 °C, 61-65%; (d) **7a**, $Pd_2(dba)_3$. Xantphos, Cs_2CO_3. dioxane, 100 °C; (ii) CF_3COOH. DCM, rt, 52-72% for two steps; (e) $SOCl_2$. MeOH, reflux, 95%.

another methoxy substituent yielded compound **24b**, which also retained good biochemical activity (8.2 nM), but the cellular potency was much reduced (118 nM). Saturation of the *N*-methyl-1-naphthamide to *N*-ethyl 3,4-dihydroquinoline-1(2H)-carboxamide **24c** led to significantly reduced potency both in the biochemical (132 nM) and cellular (118 nM) assays. Replacement of the naphthyl amide with naphthyl urea yielded compound **24d**, which retained moderate potency against FGFR1, whereas the antiproliferative effect was significantly reduced. Similar results were obtained by replacing the naphthyl amide moiety with phenylurea (**24e**).

We also attempted to replace the naphthamide moiety in **19a** with other hydrophobic functionalities, including 3,5-dimethoxyphenethyl as in **1** and 3,5-dimethoxy-2,6-dichlorophenethyl as in **3**. The corresponding compounds **24f** and **24g** completely lost the potency against FGFR1, indicating the H-bonding networks in the amido moiety of **19a** are critical. Interestingly, replacement of the naphthamido moiety with 3,5-dimethoxy-2,6-difluorobenzyl and shifting its location from C-4 to C-5 position of the central pyrimidine ring led to compound **24h** retaining moderate potency both in the biochemical (22.2 nM) and cellular (116 nM) assays. However, further substitution on this compound yielded compound **24i** that lost FGFR1 potency.

Since modification of the naphthamide moiety did not yield more potent compounds than compound **19a**. We decided to further modify the solvent interaction region that was occupied by the 3,5-dimethylpiperizin-1-yl moiety in **19a**. As shown in Table 3, various heterocyclic amines including substituted piperazines, morpholine, substituted or unsubstituted piperidines were tested. All these compounds (**25a-e**, **27**, **28**) displayed excellent potency against FGFR1 with IC_{50} values of less than 2.0 nM, although the antiproliferative effects were significantly different. The substituents on these heterocyclic amino moieties have no effects on the biochemical activity but significantly impaired the cellular potency. For example, the unsubstituted piperazine **25a** has similar biochemical activity to the 3,5-dimethylpiperazine **19a** (1.0 vs 2.1 nM), whereas the antiproliferative potency of **25a** is 4-fold more potent than **19a** (0.5 vs 14.9 nM). Similar enzymatic activity was also observed for morpholine analog **25a** and the 3,5-dimethylmorpholine **25c** (1.2 vs 1.9 nM), however, their cellular potency was 9.3 nM and 154 nM, respectively. This discrepancy may reflect the capability of cell permeability of these substituted or unsubstituted heterocyclic analogues. Further, replacement of the 3,5-dimethylpiperizin-1-yl moiety in **19a** with a Michael acceptor acrylamido moiety afforded compound **30b** retaining good biochemical potency against FGFR1 (12.8 nM), but the antiproliferative effect was significantly reduced. Compounds **35a-d** bearing a flexible alkyloxy moiety as the solvent interaction group also displayed good to high potency both in the biochemical (3.6–7.4 nM) and cellular (4.1–54 nM) assays. Based on the results above, several compounds showed high potency in the biochemical and cell proliferation assays with IC_{50} values compatible to that of the clinical FGFR1 inhibitor **1**. To evaluate the developability of this

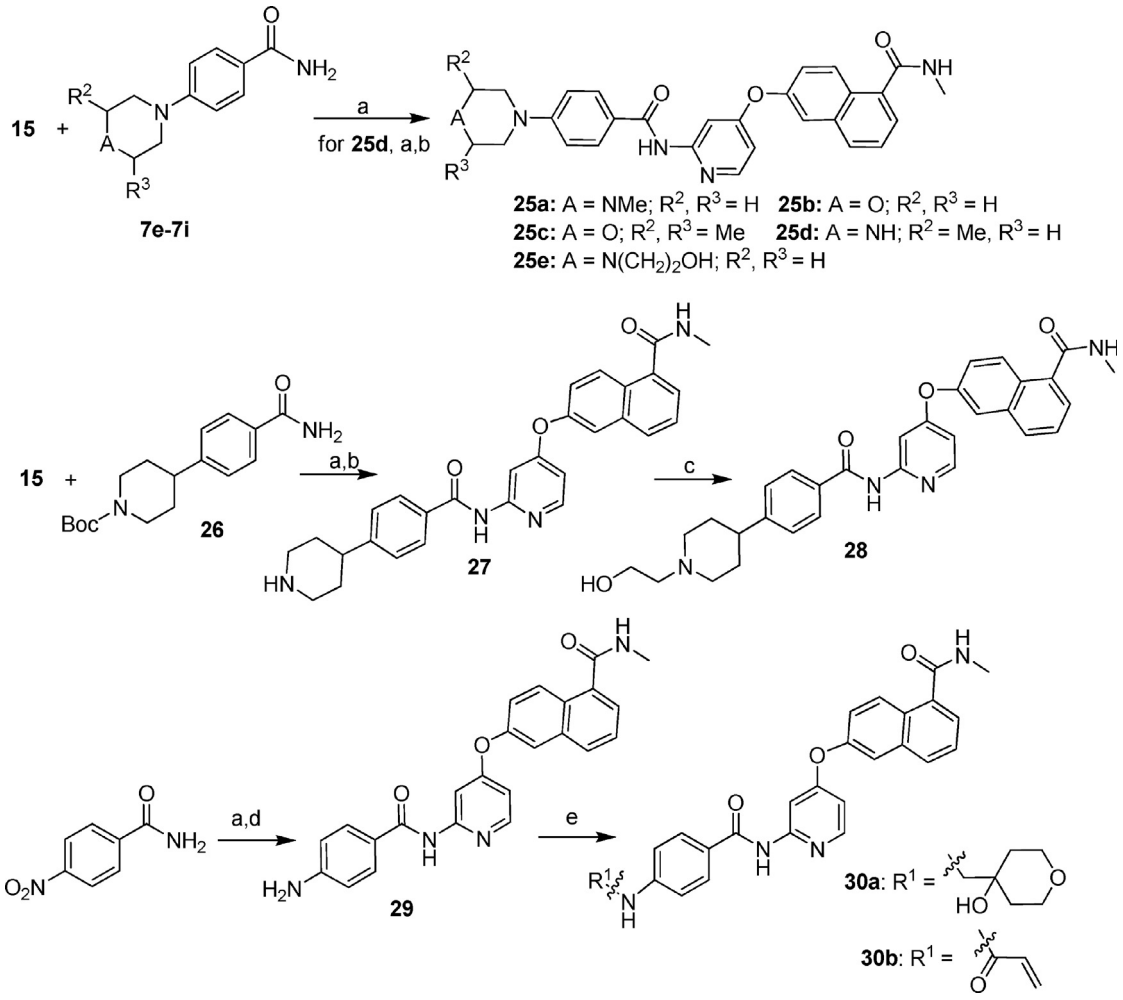

Scheme 4. *Reagents and conditions:* (a) $Pd_2(dba)_3$, Xantphos, Cs_2CO_3, dioxane, 100 °C, 49-74%; (b) CF_3COOH, DCM, 96%; (c) 2-bromoethanol, K_2CO_3, DMF, 80 °C, 62%: (d) Zn, NH_4Cl, THF/MeOH (1:1), 73.5%: (e) for **30a** 1,6-dioxaspiro[2.5]octane. DIPEA, EtOH, 32%; for **30b,** acryloyl chloride, DIPEA, dry DCM, 80%.

class compounds, we selected compound **25a** for further profiling due to its highest potency in both enzymatic and cellular assays among this series.

3.2. Molecular docking of *25a*

To elucidate the interaction mode of 2-benzamide-4-(6-oxy-*N*-methyl-1-naphthamide)-pyridine **25a** with FGFR, we conducted molecular docking analysis using a reported crystal structure of FGFR1 (PDB ID: 4RWL) [38]. As illustrated in Fig. 3, **25a** has a similar binding mode with lucitanib (**2**) and maintains the key H-bonding network observed in the complex of FGFR1 with **2**. The *N*-methyl-1-naphthamide fragment forms two hydrogen bonds with the carbonyl of the Glu531 and the NH of the Asp641 residues, and extends to the hydrophobic pocket. The 2-benzamide pyridine moiety forms a H-bonding with the NH of the Ala564 residue in the hinge region. The *N*-methyl piperazine group extends to the solvent region and forms an additional H-bonding with the carbonyl of the Glu571 upon protonizing in physiological conditions.

3.3. Kinase inhibition profile of *25a*

The selectivity profile of **25a** was evaluated against a panel of tyrosine kinases closely related to FGFR. Compared to VEGFR/FGFR dual inhibitor **2** (VEGFR1-2 IC_{50}: 7 nM and 25 nM; FGFR1-3 IC_{50}: 17.5 nM, 82.5 nM and 237.5 nM) [33], or the new released structure of the phase I clinical compound **4** (FGFR1-3 IC_{50}: 0.5–1.2 nM; VEGFR2 IC_{50}: 16 nM) [36], compound **25a** showed nearly equally high potency against FGFR1, FGFR2 and VEGFR-2 with IC_{50} values of 1.0, 4.5 and 2.9 nM, respectively (Table 4). Much lower potency was observed for other kinases tested in our experiments. The result shows that the new inhibitor **25a** is a highly potent and selective FGFR1/VEGFR2 inhibitor.

3.4. Antiproliferative activity study of *25a*

To evaluate further the antiproliferative effect of **25a** in FGFR mediated cancer cells, five aberrant FGFR cell lines were tested, including FGFR1-amplified H1581 cells, FGFR1-translocated KG1 cells, FGFR2-amplified SNU-16 cells, FGFR3-amplified RT112 cells and FGFR3-mutated UMUC14 cells. As shown in Table 5, **25a** demonstrated greater antiproliferative effects in all these FGFR1-3 subtype-selective cell lines than the selective FGFR inhibitor **1** (AZD-4547). As a FGFR/VEGFR2 dual inhibitor, **25a** also inhibited the proliferation of BAF3/VEGFR2 cell lines with an IC_{50} less than 1.5 nM.

3.5. Pharmacokinetical study of compound *25a*

The pharmacokinetical profile (PK) of the FGFR/VEGFR2 dual

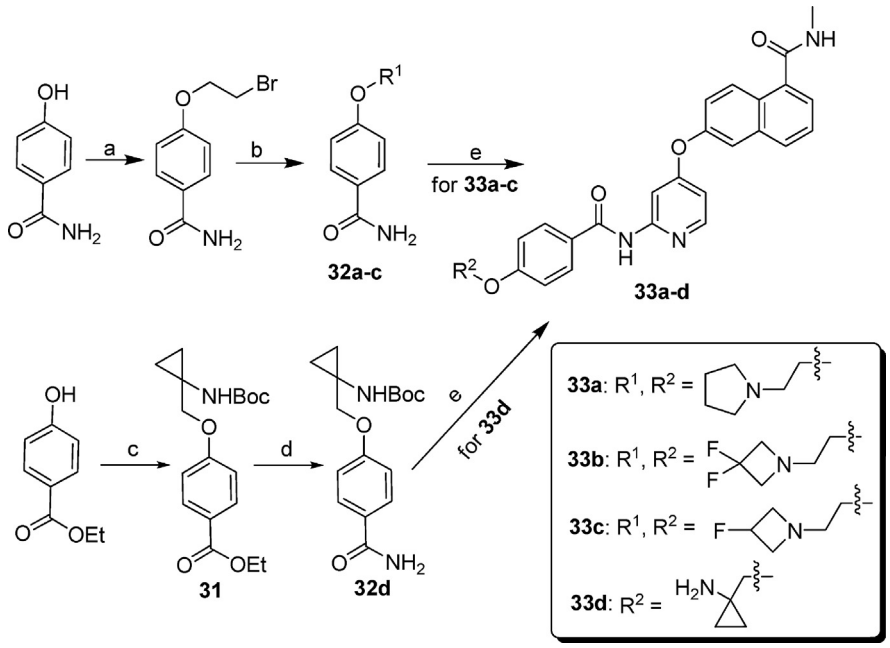

Scheme 5. *Reagents and conditions:* (a) 1,2-dibromoethane, K_2CO_3, acetone, 50 °C, N_2, 51%; (b) amines, K_2CO_3, CH_3CN, reflux, 55-62%; (c) tert-butyl 1-(iodomethyl)cyclopropylcarbamate. K_2CO_3, acetone, rt, 64%; (d) (i) NaOH, MeOH/H_2O (1:1), 60 °C; (ii) $SOCl_2$, DMF, DCM, 0 °C to rt; (iii) NH_4OH, DCM, rt, 51%; (e) for **33a-c, 15,** $Pd_2(dba)_3$, Xantphos, Cs_2CO_3, dioxane, 100 °C; for **33d,** (i) **15,** $Pd_2(dba)_3$, Xantphos, Cs_2CO_3, dioxane, 100 °C; (ii) CF_3COOH, DCM, rt, 55-67%.

inhibitor **25a** was tested in Sprague-Dawley (SD) rats dosed iv (1 mg/kg) and orally (3 mg/kg). As shown in Table 6, compound **25a** showed an acceptable half-time of 1.85 h ($T_{1/2}$) and relatively moderate oral bioavailability of 14.9%. The plasma exposure of this compound is also relatively low after both intravenous and oral administration. However, by making compound **25a** as a hydrochloride salt (with two molecular of HCl), this compound is aqueously soluble, and readily used for in vivo study.

3.6. *In vivo antitumor activity of compound **25a***

Finally, the in vivo antitumor activity of **25a** was evaluated in SNU-16 xenograft model. Compound **25a** was administered via intraperitoneal injection at doses of 10 mg/kg or 50 mg/kg once daily for 21 consecutive days. The results were demonstrated in Fig. 4. **25a** was found to suppress tumor growth in a dose-dependent manner, with tumor growth inhibition rate (TGI) of 25.0% and 81.0% at doses of 10 mg/kg and 50 mg/kg, respectively. There is no obvious body weight loss during the experiment.

4. Conclusion

In summary, starting from the phase II clinical FGFR inhibitor lucitanib (**2**), a medicinal chemistry approach was conducted by opening the quinoline fragment coupled with a scaffold hopping process thus leading a series of novel 2-benzamide-4-(6-oxy-N-methyl-1-naphthamide)-pyridine derivatives. Compound **25a** was identified to show equally high potency against FGFR1/2 and VEGFR2 with IC_{50} values less than 5.0 nM. It also suppressed the proliferation of both FGFR1/2 and VEGFR2 addictive cancer cells. *In vivo* in SNU-16 xenograft model, compound **25a** showed tumor growth inhibition rates of 25.0% and 81.0% at doses of 10 mg/kg and 50 mg/kg, respectively, without obvious body weight loss. In view of the synergistic effects of FGFs and VEGFs in tumor angiogenesis observed in preclinical studies, the selective and equally potent FGFR/VEGFR2 dual inhibitor **25a** might have better clinical benefit. This compound as its hydrochloride salt is now under our early preclinical investigation.

5. Experimental section

5.1. General methods

NMR spectral data were recorded on a Varian Mercury 300, 400 or 500 NMR spectrometer. Low-resolution mass spectra (MS) and high-resolution mass spectra (HRMS) were recorded at anionizing voltage of 70 eV on a Finnigan/MAT95 spectrometer. Column chromatography was carried out on silica gel (200–300 mesh). All reactions were monitored using thin layer chromatography (TLC) on silica gel plates. All the reagents were obtained from commercial sources, and used without further purification unless otherwise stated.

5.1.1. *6-(2-(4-((3R,5S)-3,5-dimethylpiperazin-1-yl)benzamido) pyridin-4-yloxy)-N-methyl-1-naphthamide (**19a**)*

To a mixture of **5a** (5.0 g, 32.44 mmol, 1 equiv) and (2S,6R)-2,6-dimethylpiperazine (3.7 g, 32.44 mmol, 1 equiv) in 60 mL DMSO was added K_2CO_3 (8.97 g, 64.88 mmol, 2 equiv). The mixture was heated at 110 °C for 12 h. The reaction mixture was diluted with 120 mL ice water. Ethyl acetate was added and the reaction mixture was partitioned between ethyl acetate and water. The organic phase was washed with water and brine, then dried over anhydrous Na_2SO_4, filtered and concentrated. The resulting residue was further purified via silica gel chromatography to give ethyl 4-((3R,5S)-3,5-dimethylpiperazin-1-yl)benzoate as a white solid (7.25 g, 90%). NMR (300 MHz, $CDCl_3$) δ 7.85 (d, J = 9.0 Hz, 2H), 6.79 (d, J = 9.0 Hz, 2H), 4.26 (q, J = 7.1 Hz, 2H), 3.60 (d, J = 12.0 Hz, 2H), 2.96–2.88 (m, 2H), 2.32 (t, J = 11.3 Hz, 2H), 1.30 (t, J = 7.1 Hz, 3H), 1.08 (d, J = 6.3 Hz, 6H).

The obtained methyl 4-((3R,5S)-3,5-dimethylpiperazin-1-yl) benzoate was dissolved in dichloromethane (DCM) and stirred for 15 min after adding 1 N NaOH (aq) (32.12 mL, 32.12 mmol, 1.1

Table 1
Biochemical and cellular activities of new compounds against FGFR1.

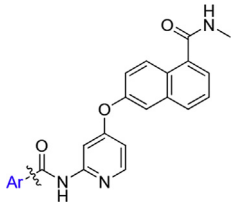

Compound	Ar	FGFR1 IC_{50} (nM)[a]	KG1 cell IC_{50} (nM)[a]
19a	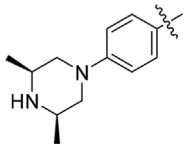	2.10 ± 0.90	14.9 ± 0.8
19b	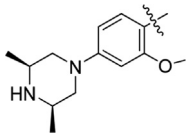	285 ± 12.7	NT[b]
19c	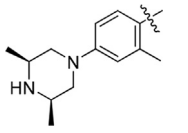	12.9 ± 0.50	>1000
19d	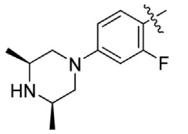	>1000	NT[b]
20	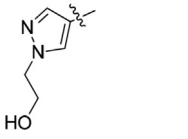	23.5 ± 3.20	278 ± 11.2
21a	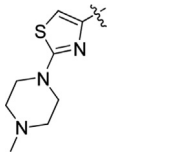	7.60 ± 3.50	NT[b]
21b	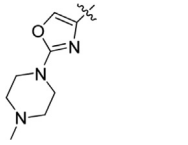	2.80 ± 0.10	NT[b]
22	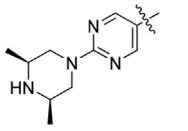	10.2 ± 3.20	30.3 ± 5.90
1(AZD-4547)	–	0.9 ± 0.3	8.7 ± 1.0

[a] Values are the mean ± SD of two independent assays.
[b] NT = not tested.

equiv). Then a solution of di-*tert*-butyl dicarbonate ester in DCM was added dropwise. The reaction mixture was stirred at room temperature until the starting material was consumed completely. The reaction mixture was then extracted with DCM and the organic phase was washed with saturated $NaHCO_3$ (aq) and brine, then dried over anhydrous Na_2SO_4, filtered and concentrated. The resulting residue was further purified via silica gel chromatography to give **6a** as colorless oil. (10.00 g, 98%). ^{1}H NMR (300 MHz, $CDCl_3$) δ 7.77 (d, J = 8.8 Hz, 2H), 6.68 (d, J = 8.7 Hz, 2H), 4.20–4.08 (m, 4H), 3.44 (d, J = 12.5 Hz, 2H), 2.87 (dd, J = 12.4, 3.8 Hz, 2H), 1.35 (s, 9H), 1.20 (t, J = 7.1 Hz, 3H), 1.14 (d, J = 6.8 Hz, 6H).

To a solution of **6a** (10.00 g, 28.70 mmol, 1 equiv) dissolved in MeOH was added 1 N NaOH (aq) (57.40 mL, 57.40 mmol, 2 equiv). The mixture was heated at 60 °C for 4 h and allowed to cool down to room temperature. The reaction mixture was acidified with 2 N HCl (aq) to adjust PH to 5–6. The resulting precipitate was collected by filtration, washed with water and dried to a constant weight to afford 4-((3R,5S)-4-(tert-butoxycarbonyl)-3,5-dimethylpiperazin-1-yl)benzoic acid (9.79 g, 98%). ^{1}H NMR (300 MHz, DMSO) δ 7.76 (d, J = 8.7 Hz, 2H), 6.97 (d, J = 8.9 Hz, 2H), 4.18–4.05 (m, 2H), 3.75 (d, J = 12.8 Hz, 2H), 2.98 (dd, J = 12.9, 4.3 Hz, 2H), 1.42 (s, 9H), 1.19 (d, J = 6.7 Hz, 6H).

The obtained acid (9.79 g, 29.28 mmol, 1 equiv) was dissolved in dry DCM and allowed to cool down to 0 °C. DMF (22.57 mL, 292.8 mmol, 10equiv) and thionyl chloride (4.25 mL, 58.56 mmol, 2 equiv) dissolved in dry DCM were added dropwise to the mixture above. Then the reaction mixture was allowed to warm up to room temperature slowly and left to stir for 2 h. The solvent was removed under reduced pressure at room temperature. Then the residue was redissolved in dry DCM, and was added to the DCM solution of NH_4OH (11.28 mL 292.8 mmol, 10 equiv), which was cooled down to 0 °C already. The ice-bath was removed and the reaction mixture was stirred at room temperature for 4 h. The reaction mixture was then extracted with DCM and the organic phase was washed with saturated $NaHCO_3$ (aq) and brine, then dried over anhydrous Na_2SO_4, filtered and concentrated. The resulting residue was further purified via silica gel chromatography to give **7a** as a white solid (4.88 g, 50%). ^{1}H NMR (300 MHz, $CDCl_3$) δ 7.67 (d, J = 8.5 Hz, 2H), 6.81 (d, J = 8.7 Hz, 2H), 5.87 (s, 2H), 4.29–4.10 (m, 2H), 3.50 (d, J = 12.3 Hz, 2H), 2.97 (dd, J = 12.3, 3.8 Hz, 2H), 1.43 (s, 9H), 1.25 (d, J = 6.8 Hz, 6H).

14 (8.0 g, 26.69 mmol, 1 equiv), methylamine hydrochloride (2.7 g, 40.04 mmol, 1.5 equiv), EDCI (7.68 g, 40.04 mmol, 1.5 equiv), HOBt (3.61 g, 26.69 mmol, 1.0 equiv) and DIPEA (11.02 mL, 66.72 mmol, 2.5 equiv) were dissolved in dry DCM and the reaction mixture was left to stir at room temperature overnight. The reaction mixture was then extracted with DCM and the organic phase was washed with saturated $NaHCO_3$ (aq) and brine, then dried over anhydrous Na_2SO_4, filtered and concentrated. The resulting residue was further purified via silica gel chromatography to give **15** as white solid (8.0 g, 95.8%). ^{1}H NMR (300 MHz, $CDCl_3$) δ 8.40 (d, J = 9.2 Hz, 1H), 8.18 (d, J = 5.5 Hz, 1H), 7.81 (d, J = 8.3 Hz, 1H), 7.55 (d, J = 6.8 Hz, 1H), 7.51–7.42 (m, 2H), 7.24 (dd, J = 9.3, 2.3 Hz, 1H), 6.78 (d, J = 7.6 Hz, 2H), 6.05 (d, J = 4.0 Hz, 1H), 3.05 (d, J = 4.9 Hz, 3H).

7a (100 mg, 0.30 mmol, 1 equiv) and **15** (112.56 mg, 0.36 mmol, 1.2 equiv) were dissolved in 10 mL dry dioxane. Then $Pd_2(dba)_3$ (27.47 mg, 0.03 mmol, 0.1 equiv), Xantphos (34.72 mg, 0.06 mmol, 0.2 equiv) and Cs_2CO_3 (195.49 mg, 0.60 mmol, 2 equiv) were added to the mixture above. The reaction mixture was left to stir at 110 °C for 5 h under nitrogen atmosphere. The reaction mixture was then extracted with DCM and the organic phase was washed with saturated $NaHCO_3$ (aq) and brine, then dried over anhydrous Na_2SO_4, filtered and concentrated. The resulting residue was further purified via silica gel chromatography to give (2S,6R)-*tert*-butyl 2,6-dimethyl-4-(4-(4-(5-(methylcarbamoyl)naphthalen-2-yloxy)pyridin-2-ylcarbamoyl)phenyl)piperazine-1-carboxylate, which was redissolved in methanol solution of 2 N HCl. The reaction mixture was left to stir at room temperature for 2 h. Then the reaction mixture was basified with sodium bicarbonate to adjust

Table 2
Biochemical and cellular activities of new compounds against FGFR1.11

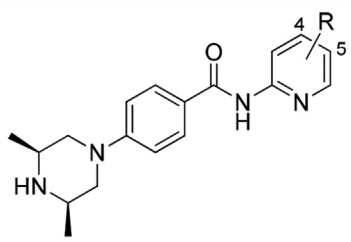

Compound	4-	5-	FGFR1 IC_{50} (nM)[a]	KG1 cell IC_{50} (nM)[a]
24a	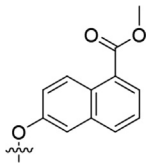	H	4.6 ± 0.4	159 ± 27.4
24b	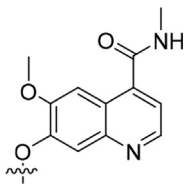	H	8.2 ± 2.5	>1000
24c	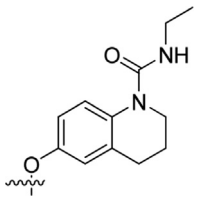	H	132 ± 9.4	118 ± 19.7
24d	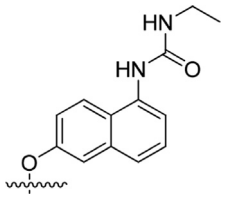	H	67.5 ± 31.3	504 ± 279
24e	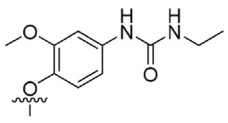	H	36.1 ± 3.8	548 ± 303
24f	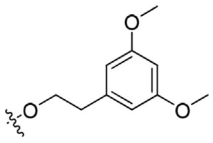	H	>1000	NT[b]
24g	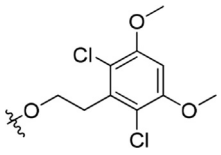	H	>1000	NT[b]
24h	H	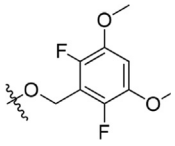	22.2 ± 0.7	116 ± 9.5

(*continued on next page*)

Table 2 (*continued*)

Compound	4-	5-	FGFR1 IC_{50} (nM)[a]	KG1 cell IC_{50} (nM)[a]
24i	H	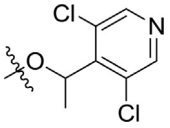	>1000	NT[b]

[a] Values are the mean ± SD of two independent assays.
[b] NT = not tested.

pH to 7–8. The reaction mixture was then extracted with DCM and the organic phase was washed with saturated $NaHCO_3$ (aq) and brine, then dried over anhydrous Na_2SO_4, filtered and concentrated. The resulting residue was further purified via silica gel chromatography to give **19a** as white solid (106 mg, 58% for two steps). ^{1}H NMR (300 MHz, $CDCl_3$) δ 8.45 (s, 1H), 8.34 (d, *J* = 9.2 Hz, 1H), 8.09 (d, *J* = 5.7 Hz, 1H), 7.97 (d, *J* = 1.3 Hz, 1H), 7.79 (d, *J* = 8.1 Hz, 1H), 7.70 (d, *J* = 8.6 Hz, 2H), 7.50 (s, 2H), 7.41 (t, *J* = 7.6 Hz, 1H), 7.29 (dd, *J* = 9.1, 1.7 Hz, 1H), 6.83 (d, *J* = 8.7 Hz, 2H), 6.60 (dd, *J* = 5.6, 1.5 Hz, 1H), 6.07 (d, *J* = 4.3 Hz, 1H), 3.61 (d, *J* = 11.1 Hz, 2H), 3.03 (d, *J* = 4.7 Hz, 3H), 2.94 (s, 2H), 2.35 (t, *J* = 11.2 Hz, 2H), 1.10 (d, *J* = 6.2 Hz, 6H). ^{13}C NMR (126 MHz, $CDCl_3$) δ 170.06, 166.33, 165.30, 153.75, 153.64, 152.24, 149.15, 134.78, 134.76, 129.99, 128.82, 128.27, 127.90, 125.76, 124.52, 122.66, 121.49, 117.56, 113.95, 108.94, 102.31, 54.34, 50.44, 26.83, 19.68. MS (ESI) *m/z* 510.40 $[M + H]^+$. HRMS: calcd for $C_{30}H_{32}N_5O_3$ $[M + H]^+$, 510.2500; found 510.2513.

5.1.2. 6-(2-(4-((3R,5S)-3,5-dimethylpiperazin-1-yl)-2-methoxybenzamido)pyridin-4-yloxy)-N-methyl-1-naphthamide (**19b**)

7b was obtained according to the similar procedure of preparing **7a** starting from **5b**. White solid; yield 39%; ^{1}H NMR (300 MHz, $CDCl_3$) δ 8.09 (d, *J* = 8.9 Hz, 1H), 7.57 (s, 1H), 6.56 (d, *J* = 8.9 Hz, 1H), 6.35 (s, 1H), 5.64 (s, 1H), 4.34–4.19 (m, 2H), 3.96 (s, 3H), 3.57 (d, *J* = 12.5 Hz, 2H), 3.08 (dd, *J* = 12.5, 4.3 Hz, 2H), 1.49 (s, 9H), 1.32 (d, *J* = 6.8 Hz, 6H).

19b was obtained according to the similar procedure of preparing **19a** using **15** and **7b**. White solid; yield 49%; ^{1}H NMR (300 MHz, $CDCl_3$) δ 10.28 (s, 1H), 8.37 (d, *J* = 9.1 Hz, 1H), 8.17 (d, *J* = 5.7 Hz, 1H), 8.10 (d, *J* = 1.9 Hz, 1H), 7.99 (d, *J* = 8.9 Hz, 1H), 7.83 (d, *J* = 8.1 Hz, 1H), 7.54 (d, *J* = 6.5 Hz, 2H), 7.44 (t, *J* = 7.6 Hz, 1H), 7.34 (dd, *J* = 9.3, 2.1 Hz, 1H), 6.63 (dd, *J* = 5.6, 2.0 Hz, 1H), 6.53 (dd, *J* = 9.2, 1.4 Hz, 1H), 6.37 (s, 1H), 6.24 (d, *J* = 5.0 Hz, 1H), 4.06 (s, 3H), 3.64 (d, *J* = 10.1 Hz, 2H), 3.06 (d, *J* = 4.8 Hz, 3H), 3.03–2.93 (m, 2H), 2.41 (t, *J* = 11.2 Hz, 2H), 1.15 (d, *J* = 6.3 Hz, 6H). ^{13}C NMR (126 MHz, $CDCl_3$) δ 170.28, 166.25, 163.95, 159.26, 155.23, 154.30, 152.54, 149.36, 134.90, 133.71, 130.09, 128.32, 127.95, 125.87, 124.63, 121.65, 117.58, 110.93, 108.86, 107.68, 103.07, 97.04, 56.15, 54.43, 50.65, 26.97, 19.76. MS (ESI) *m/z* 540.30 $[M + H]^+$. HRMS: calcd for $C_{31}H_{34}N_5O_4$ $[M + H]^+$, 540.2605; found 540.2610.

5.1.3. 6-(2-(4-((3R,5S)-3,5-dimethylpiperazin-1-yl)-2-methylbenzamido)pyridin-4-yloxy)-N-methyl-1-naphthamide (**19c**)

7c was obtained according to the similar procedure of preparing **7a** starting from **5c**. White solid; yield 33%; ^{1}H NMR (300 MHz, $CDCl_3$) δ 7.44 (d, *J* = 8.6 Hz, 1H), 6.70 (d, *J* = 7.2 Hz, 2H), 5.69 (s, 2H), 4.31–4.19 (m, 2H), 3.49 (d, *J* = 11.9 Hz, 2H), 2.96 (dd, *J* = 12.3, 4.1 Hz, 2H), 2.52 (s, 3H), 1.49 (s, 9H), 1.32 (d, *J* = 6.8 Hz, 6H).

19c was obtained according to the similar procedure of preparing **19a** using **15** and **7c**. White solid; yield 52%; ^{1}H NMR (300 MHz, $CDCl_3$) δ 8.28 (d, *J* = 9.2 Hz, 1H), 8.04 (d, *J* = 5.8 Hz, 1H), 7.89 (s, 1H), 7.80 (d, *J* = 8.1 Hz, 1H), 7.53 (d, *J* = 6.9 Hz, 2H), 7.42 (dd, *J* = 13.3, 7.9 Hz, 2H), 7.30 (s, 1H), 6.64 (dd, *J* = 13.9, 7.0 Hz, 3H), 3.57 (d, *J* = 10.9 Hz, 2H), 2.99 (s, 3H), 2.96–2.91 (m, 2H), 2.40 (s, 3H), 2.30 (t, *J* = 11.3 Hz, 2H), 1.10 (d, *J* = 6.3 Hz, 6H). ^{13}C NMR (126 MHz, $CDCl_3$) δ 174.85, 172.52, 170.53, 157.50, 156.45, 155.94, 152.96, 143.04, 138.64, 138.46, 133.92, 132.92, 132.10, 131.80, 129.82, 128.80, 125.33, 121.58, 121.55, 116.06, 112.92, 106.45, 58.31, 54.34, 33.58, 30.49, 24.69, 22.91. MS (ESI) *m/z* 524.20 $[M + H]^+$. HRMS: calcd for $C_{31}H_{34}N_5O_3$ $[M + H]^+$, 524.2656; found 524.2670.

5.1.4. 6-(2-(4-((3R,5S)-3,5-dimethylpiperazin-1-yl)-2-fluorobenzamido)pyridin-4-yloxy)-N-methyl-1-naphthamide (**19d**)

7d was obtained according to the similar procedure of preparing **7a** starting from **5d**. White solid; yield 37%; ^{1}H NMR (300 MHz, $CDCl_3$) δ 8.78 (s, 1H), 8.11–8.01 (m, 1H), 6.88 (d, *J* = 9.6 Hz, 2H), 5.97 (s, 1H), 4.32–4.16 (m, 2H), 2.87 (dt, *J* = 11.6, 7.9 Hz, 4H), 1.43 (s, 9H), 1.32 (d, *J* = 7.0 Hz, 6H).

19d was obtained according to the similar procedure of preparing **19a** using **15** and **7d**. White solid; yield 58%; ^{1}H NMR (300 MHz, DMSO) δ 12.56 (s, 1H), 8.54 (d, *J* = 4.6 Hz, 1H), 8.35 (d, *J* = 9.2 Hz, 1H), 8.29 (d, *J* = 5.7 Hz, 1H), 8.01 (dd, *J* = 15.5, 8.2 Hz, 2H), 7.89 (s, 1H), 7.83 (d, *J* = 1.9 Hz, 1H), 7.67–7.55 (m, 2H), 7.46 (dd, *J* = 9.3, 2.1 Hz, 1H), 7.26 (dd, *J* = 10.8, 2.0 Hz, 1H), 7.09 (t, *J* = 8.3 Hz, 1H), 6.83 (dd, *J* = 5.8, 1.9 Hz, 1H), 3.22 (s, 2H), 3.00 (d, *J* = 10.1 Hz, 2H), 2.87 (d, *J* = 3.5 Hz, 3H), 2.44 (t, *J* = 10.6 Hz, 2H), 0.99 (d, *J* = 6.1 Hz, 6H). ^{13}C NMR (126 MHz, DMSO) δ 168.83, 165.60,164.70 (d, *J* = 252 Hz), 163.27, 153.78 (d, *J* = 8.8 Hz), 153.69, 151.42, 150.15, 134.64 (d, *J* = 84.4 Hz), 133.41 (d, *J* = 10.1 Hz), 129.44, 128.44, 127.60, 126.11, 124.92, 123.38 (d, *J* = 2.5 Hz), 121.27, 117.62, 111.72 (d, *J* = 21.4 Hz), 109.16 (d, *J* = 23.9 Hz), 108.86, 101.42, 59.38, 50.00, 26.22, 18.84. MS (ESI) *m/z* 528.30 $[M + H]^+$. HRMS: calcd for $C_{30}H_{31}FN_5O_3$ $[M + H]^+$, 528.2405; found 528.2418.

5.1.5. 1-(2-hydroxyethyl)-N-(4-(5-(methylcarbamoyl)naphthalen-2-yloxy)pyridin-2-yl)-1H-pyrazole-4-carboxamide (**20**)

16 (362 mg, 1.00 mmol, 2 equiv), **17** (56 mg, 0.50 mmol, 1 equiv) and K_2CO_3 (138 mg, 1.00 mmol, 2 equiv) dissolved in DMF were heated at 60 °C overnight. The reaction mixture was then extracted with ethyl acetate and the organic phase was washed with saturated $NaHCO_3$ (aq) and brine, then dried over anhydrous Na_2SO_4, filtered and concentrated. The resulting residue was further purified via silica gel chromatography to give **18** as white solid (124 mg, 63%). ^{1}H NMR (300 MHz, $CDCl_3$) δ 7.94 (s, 1H), 7.79 (s, 1H), 7.52–7.50 (m, 4H), 7.42–7.33 (m, 6H), 5.61 (s, 2H), 4.24 (t, *J* = 4.9 Hz, 2H), 3.98 (t, *J* = 5.0 Hz, 2H), 1.00 (s, 9H).

18 (116 mg, 0.30 mmol, 1 equiv) and **15** (112 mg, 0.36 mmol, 1.2 equiv) were dissolved in 10 mL dry dioxane. Then $Pd_2(dba)_3$ (27 mg, 0.03 mmol, 0.1 equiv), Xantphos (34 mg, 0.06 mmol, 0.2 equiv) and Cs_2CO_3 (195 mg, 0.60 mmol, 2 equiv) were added to the mixture above. The reaction mixture was left to stir at 110 °C for 5 h under nitrogen atmosphere. The reaction mixture was then extracted with DCM and the organic phase was washed with saturated $NaHCO_3$ (aq) and brine, then dried over anhydrous Na_2SO_4, filtered and concentrated. The resulting residue was further purified via silica gel chromatography to give 1-(2-(tert-butyldiphenylsilyloxy) ethyl)-N-(4-(5-(methylcarbamoyl)naphthalen-2-yloxy)pyridin-2-yl)–pyrazole-4-carboxamide as white solid (131 mg, 65%). ^{1}H NMR

Table 3
Biochemical and cellular activities of new compounds against FGFR1.21

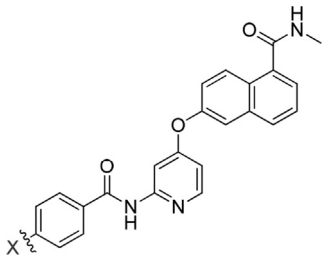

Compound	X	FGFR1 IC_{50}, nM[a]	KG1 cell IC_{50}, nM (%)[a]
25a	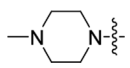	1.0 ± 0.3	<0.5
25b	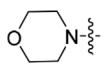	1.2 ± 0.3	9.3 ± 4.9
25c	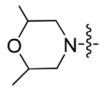	1.9 ± 0.7	154 ± 35.6
25d	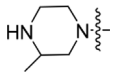	2.0 ± 0.5	<4.1
25e	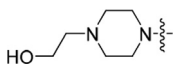	1.9 ± 0.3	5.8 ± 0.3
27	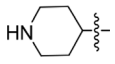	1.6 ± 0.6	72.2 ± 7.2
28	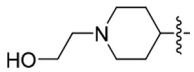	1.2 ± 0.2	<4.1
30a	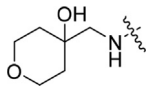	6.2 ± 0.5	<4.1
30b	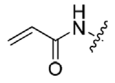	12.8 ± 2.5	369 ± 31.5
33a	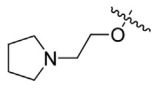	4.1 ± 0.8	<4.1
33b	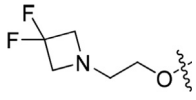	6.1 ± 1.4	<4.1
33c	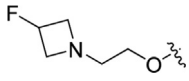	3.6 ± 0.1	5.1 ± 0.5
33d	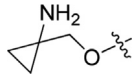	7.4 ± 0.6	54.5 ± 8.6

[a] Values are the mean ± SD of two independent assays.

(300 MHz, $CDCl_3$) δ 8.35 (d, J = 9.2 Hz, 1H), 8.20 (s, 1H), 8.09 (d, J = 5.5 Hz, 1H), 7.93 (s, 2H), 7.86–7.76 (m, 2H), 7.52 (d, J = 6.5 Hz, 2H), 7.45 (d, J = 7.1 Hz, 4H), 7.42–7.24 (m, 8H), 6.60 (d, J = 5.7 Hz, 1H), 6.07 (d, J = 5.1 Hz, 1H), 4.18 (t, J = 4.7 Hz, 2H), 3.92 (t, J = 4.8 Hz, 2H), 3.04 (d, J = 4.8 Hz, 3H), 0.93 (s, 9H).

The intermediate obtained above (131 mg, 0.20 mmol, 1 equiv) and CsF (89 mg, 0.59 mmol, 3 equiv) dissolved in DMF were heated at 80 °C overnight. The reaction mixture was then extracted with ethyl acetate and the organic phase was washed with saturated $NaHCO_3$ (aq) and brine, then dried over anhydrous Na_2SO_4, filtered and concentrated. The resulting residue was further purified via silica gel chromatography to give **20** as white solid (35 mg, 42%). ^{1}H NMR (300 MHz, DMSO) δ 10.59 (s, 1H), 8.53 (d, J = 4.6 Hz, 1H), 8.43 (s, 1H), 8.33 (d, J = 9.3 Hz, 1H), 8.27 (d, J = 5.6 Hz, 1H), 8.09 (s, 1H), 8.02 (dd, J = 7.1, 1.5 Hz, 1H), 7.82 (d, J = 8.3 Hz, 2H), 7.64–7.53 (m, 2H), 7.45 (dd, J = 9.2, 1.7 Hz, 1H), 6.80 (d, J = 5.7 Hz, 1H), 4.14 (t, J = 5.4 Hz, 2H), 3.72 (t, J = 5.2 Hz, 2H), 2.86 (d, J = 4.1 Hz, 3H). ^{13}C NMR (126 MHz, DMSO) δ 169.29, 165.84, 161.59, 154.72, 151.93, 149.99, 139.94, 135.43, 134.75, 133.57, 129.86, 128.80, 127.97, 126.52, 125.30, 121.73, 117.99, 117.89, 108.98, 102.12, 60.09, 54.93, 26.66. MS (ESI) m/z 432.30 $[M + H]^+$. HRMS: calcd for $C_{23}H_{22}N_5O_4$ $[M + H]^+$, 432.1666; found 432.1668.

*5.1.6. N-(4-(5-(methylcarbamoyl)naphthalen-2-yloxy)pyridin-2-yl)-2-(4-methylpiperazin-1-yl)thiazole-4-carboxamide (**21a**)*

8a (888 mg, 4.00 mmol, 1 equiv), 1-methylpiperazine (0.66 mL, 6.00 mmol, 1.5 equiv) and K_2CO_3 (828 mg, 6.00 mmol, 1.5 equiv) dissolved in CH_3CN were heated at 80 °C for 3 h. The reaction mixture was then extracted with DCM and the organic phase was washed with saturated $NaHCO_3$ (aq) and brine, then dried over anhydrous Na_2SO_4, filtered and concentrated. The resulting residue was further purified via silica gel chromatography to give **9a** as a yellowish-brown grease (710 mg, 70%). ^{1}H NMR (300 MHz, $CDCl_3$) δ 8.11 (s, 1H), 4.28 (q, J = 7.1 Hz, 2H), 3.64–3.50 (m, 4H), 2.58–2.44 (m, 4H), 2.34 (s, 3H), 1.33 (t, J = 7.1 Hz, 3H).

To a solution of **9a** (690 mg, 2.88 mmol, 1 equiv) dissolved in MeOH was added 1 N NaOH (aq) (5.76 mL, 5.76 mmol, 2 equiv). The reaction mixture was heated at 60 °C for 2 h and was allowed to cool down to room temperature. The residue was acidified with 2 N HCl (aq) to adjust PH to 5–6. Then the solvent was removed under reduced pressure to obtain the crude acid for next step. The obtained acid (653 mg in theory, 2.88 mmol, 1 equiv) was dissolved in dry DCM and was allowed to cool down to 0 °C. DMF (2.22 mL, 28.8 mmol, 10equiv) and thionyl chloride (0.82 mL, 11.52 mmol, 4 equiv) dissolved in dry DCM were added dropwise to the mixture above. Then the reaction mixture was allowed to warm up to room temperature slowly and was left to stir for 2 h. The solvent was removed under reduced pressure at room temperature. Then the residue was redissolved in dry DCM, and was added to the DCM solution of NH_4OH (1.11 mL, 28.8 mmol, 10 equiv), which was allowed to cool down to 0 °C already. The ice-bath was removed and the reaction mixture was left to stir at room temperature for 4 h. The reaction mixture was then extracted with DCM and the organic phase was washed with saturated $NaHCO_3$ (aq) and brine, then dried over anhydrous Na_2SO_4, filtered and concentrated. The resulting residue was further purified via silica gel chromatography to give **10a** (456 mg, 70%). ^{1}H NMR (300 MHz, $CDCl_3$) δ 7.42 (s, 1H), 7.01 (s, 1H), 5.73 (s, 1H), 3.58–3.44 (m, 4H), 2.57–2.46 (m, 4H), 2.35 (s, 3H).

21a was obtained according to the similar procedure of preparing **19a** using **15** and **10a**. White solid; yield 69%; ^{1}H NMR (300 MHz, $CDCl_3$) δ 9.61 (s, 1H), 8.40 (d, J = 9.0 Hz, 1H), 8.19 (d, J = 5.6 Hz, 1H), 8.02 (d, J = 1.8 Hz, 1H), 7.85 (d, J = 8.2 Hz, 1H), 7.57 (d, J = 7.0 Hz, 2H), 7.52–7.44 (m, 1H), 7.42 (s, 1H), 7.35 (dd, J = 9.2, 2.3 Hz, 1H), 6.67 (dd, J = 5.7, 2.1 Hz, 1H), 6.08 (d, J = 4.1 Hz, 1H), 3.63–3.51 (m, 4H), 3.10 (d, J = 4.9 Hz, 3H), 2.58–2.48 (m, 4H). ^{13}C NMR (126 MHz, $CDCl_3$) δ 170.40, 170.03, 166.28, 159.65, 153.10, 152.25, 149.39, 145.86, 134.79, 130.06, 128.27, 127.92, 125.77, 124.49, 121.55, 117.58, 113.38, 109.10, 102.30, 54.07, 48.29, 46.17, 26.87. MS (ESI) m/z 503.32 $[M + H]^+$. HRMS: calcd for $C_{26}H_{27}N_6O_3S$ $[M + H]^+$, 503.1860; found 503.1872.

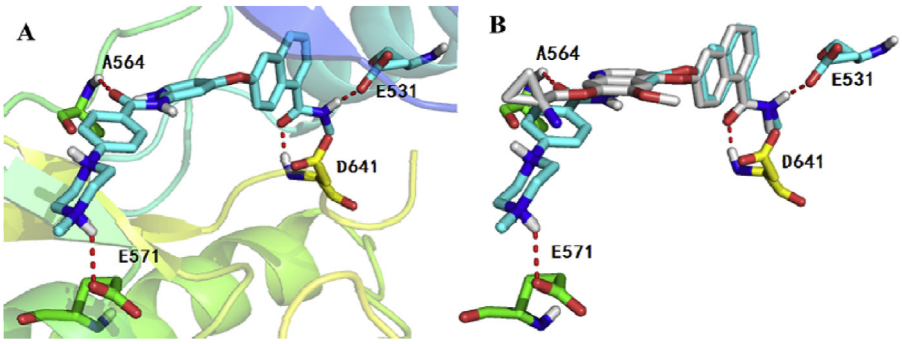

Fig. 3. The molecular docking study of FGFR1 with **25a** (A) and **2** (B). The atoms of **25a** are colored as follows: carbon, light blue; oxygen, red; nitrogen, blue; hydrogen, white. Hydrogen bonds are shown as red dashed lines to the key residues (Glu531, Asp641, Ala564 and Glu571). The protein is shown as a cartoon and key residues are shown as sticks. The atoms of compounds are colored as follows: carbon, grey; oxygen, red; nitrogen, blue; hydrogen, white. (For interpretation of the references to color in this figure legend, the reader is referred to the Web version of this article.)

Table 4
Kinase-selectivity profile of **25a.**

Tyrosine kinase[a]	IC_{50} (nM)[b]	Tyrosine kinase[a]	IC_{50} (nM)[b]
FGFR1	1.0 ± 0.3	FLT-3	>1000
FGFR2	4.5 ± 0.7	EGFR	>1000
FGFR3	10.6 ± 0.4	ErbB2	>1000
FGFR4	>1000	ErbB4	>1000
VEGFR2	2.9 ± 0.4	c-Src	>1000
VEGFR1	79.3%@10 nM	Bcr-Abl	>1000
PDGFRα	44.1%@10 nM	EPH-A2	>1000
PDGFRβ	59.5%@100 nM	IGF1R	>1000
c-KIT	54.7%@10 nM	–	–

[a] EGFR, epidermal growth factor receptor; VEGFR, vascular endothelial growth factor; PDGFR, platelet derived growth factor receptor; c-Kit, stem cell factor receptor; Flt, fms-like tyrosine kinase; c-Src, cellular Src kinase; Bcr-Abl, breakpoint cluster region-abelson; EPHA, erythropoietin-producing hepatocellular carcinoma receptor.
[b] Values are the mean ± SD of three independent assays.

Table 5
Antiproliferative activity of **25a** on FGFR addicted cells and BAF3/VEGFR-2 cells.

Cell Lines	IC_{50} (nM)[a]	
	25a (SOMCL-286)	1 (AZD4547)
H1581 (FGFR1)	22.3 ± 0.0	40.0 ± 2.8
KG1 (FGFR1)	<0.5	1.9 ± 0.0
SNU16 (FGFR2)	<0.5	6.2 ± 1.4
RT112 (FGFR3)	52.6 ± 28.1	83.8 ± 12.5
UMUC14 (FGFR3)	1.7 ± 0.2	26.9 ± 0.2
BAF3/VEGFR-2	<1.5	222 ± 33.8

[a] Values are the mean ± SD of two independent assays.

*5.1.7. N-(4-(5-(methylcarbamoyl)naphthalen-2-yloxy)pyridin-2-yl)-2-(4-methylpiperazin-1-yl)oxazole-4-carboxamide (**21b**)*

10b was obtained according to the similar procedure of preparing **10a** starting from **8b**. White solid; yield 40%; ^{1}H NMR (300 MHz, $CDCl_3$) δ 7.76 (s, 1H), 6.71 (s, 1H), 5.70 (s, 1H), 3.56–3.49 (m, 4H), 2.52–2.42 (m, 4H), 2.33 (s, 3H).

21b was obtained according to the similar procedure of preparing **19a** using **15** and **10b**. Light yellow solid; yield 55%; ^{1}H NMR (300 MHz, $CDCl_3$) δ 9.20 (s, 1H), 8.35 (d, J = 9.2 Hz, 1H), 8.13 (d, J = 5.6 Hz, 1H), 7.92 (d, J = 1.7 Hz, 1H), 7.79 (d, J = 8.2 Hz, 1H), 7.71 (s, 1H), 7.52 (d, J = 7.1 Hz, 2H), 7.46–7.38 (m, 1H), 7.29 (dd, J = 9.3, 2.1 Hz, 1H), 6.61 (dd, J = 5.8, 2.0 Hz, 1H), 6.01 (d, J = 3.5 Hz, 1H), 3.55–3.44 (m, 4H), 3.04 (d, J = 4.8 Hz, 3H), 2.47–2.37 (m, 4H), 2.29 (s, 3H). ^{13}C NMR (126 MHz, $CDCl_3$) δ 170.01, 166.26, 160.66, 159.65, 152.84, 152.20, 149.40, 135.59, 135.55, 134.78, 130.05, 128.28, 127.93, 125.77, 124.50, 121.54, 117.60, 109.14, 102.31, 54.04, 46.21, 45.53, 26.87. MS (ESI) m/z 487.35 $[M + H]^+$. HRMS: calcd for $C_{26}H_{27}N_6O_4$ $[M + H]^+$, 487.2088; found 487.2078.

*5.1.8. 2-((3R,5S)-3,5-dimethylpiperazin-1-yl)-N-(4-(5-(methylcarbamoyl)naphthalene-2-yloxy)pyridin-2-yl)pyrimidine-5-carboxamide (**22**)*

13 was obtained according to the similar procedure of preparing **7a** starting from **11** and (2R,6S)-2,6-dimethylpiperazine. Light yellow solid; yield 44%; ^{1}H NMR (300 MHz, $CDCl_3$) δ 8.72 (s, 2H), 5.68 (s, 2H), 4.71 (d, J = 13.2 Hz, 2H), 4.39–4.21 (m, 2H), 3.17 (dd, J = 13.0, 4.5 Hz, 2H), 1.49 (s, 9H), 1.19 (d, J = 6.9 Hz, 6H).

22 was obtained according to the similar procedure of preparing **19a** using **15** and **13.** Light yellow solid; yield 51%; ^{1}H NMR (300 MHz, $CDCl_3$) δ 8.76 (s, 2H), 8.55 (s, 1H), 8.39 (d, J = 9.2 Hz, 1H), 8.13 (d, J = 5.7 Hz, 1H), 7.96 (d, J = 1.8 Hz, 1H), 7.84 (d, J = 8.1 Hz, 1H), 7.56 (d, J = 6.3 Hz, 2H), 7.51–7.43 (m, 1H), 7.32 (dd, J = 9.2, 2.3 Hz, 1H), 6.67 (dd, J = 5.7, 2.1 Hz, 1H), 6.20 (d, J = 4.9 Hz, 1H), 4.76 (d, J = 11.6 Hz, 2H), 3.08 (d, J = 4.8 Hz, 3H), 2.87 (s, 2H), 2.59–2.47 (m, 2H), 1.15 (d, J = 6.2 Hz, 6H). ^{13}C NMR (126 MHz, $CDCl_3$) δ 170.17, 166.54, 163.04, 161.86, 157.80, 153.39, 152.32, 149.36, 134.93, 130.21, 128.50, 128.10, 125.97, 124.69, 121.61, 117.74, 115.29, 109.42, 102.85, 50.94, 50.57, 27.05, 19.61. MS (ESI) m/z 512.30 $[M + H]^+$. HRMS: calcd for $C_{28}H_{30}N_7O_3$ $[M + H]^+$, 512.2405; found 512.2398.

*5.1.9. Methyl 6-(2-(4-((3R,5S)-3,5-dimethylpiperazin-1-yl) benzamido)pyridin-4- yloxy)-1-naphthoate (**24a**)*

14 (100 mg, 0.33 mmol, 1 equiv) and thionyl chloride (0.05 mL, 0.66 mmol, 2 equiv) were dissolved in anhydrous MeOH. The reaction mixture was refluxed overnight. Then the solvent was

Table 6
Pharmacokinetics profile of **25a** in SD rats.[a]

Route	$T_{1/2}$ (h)	AUC_{last} (h.ng/mL)	AUC_{INF_obs} (h.ng/mL)	$CL_{\_obs}$ (mL/min/kg)	$Vss_{\_obs}$ (mL/kg)	F (%)
Po (3 mg/kg)	1.85	21.4	22.7	–	–	14.9
Iv (1 mg/kg)	0.897	47.9	49.0	346	16,694	

[a] Values are the average of three runs. Vehicle: PO: DMSO/0.5%HPMC (5/95, v/v); iv: EtOH/PEG300/NaCl (10/40/50, v/v/v). CL, clearance; Vss, volume of distribution; $T_{1/2}$, half-life; AUC, area under the plasma concentration time curve; F, oral bioavailability.

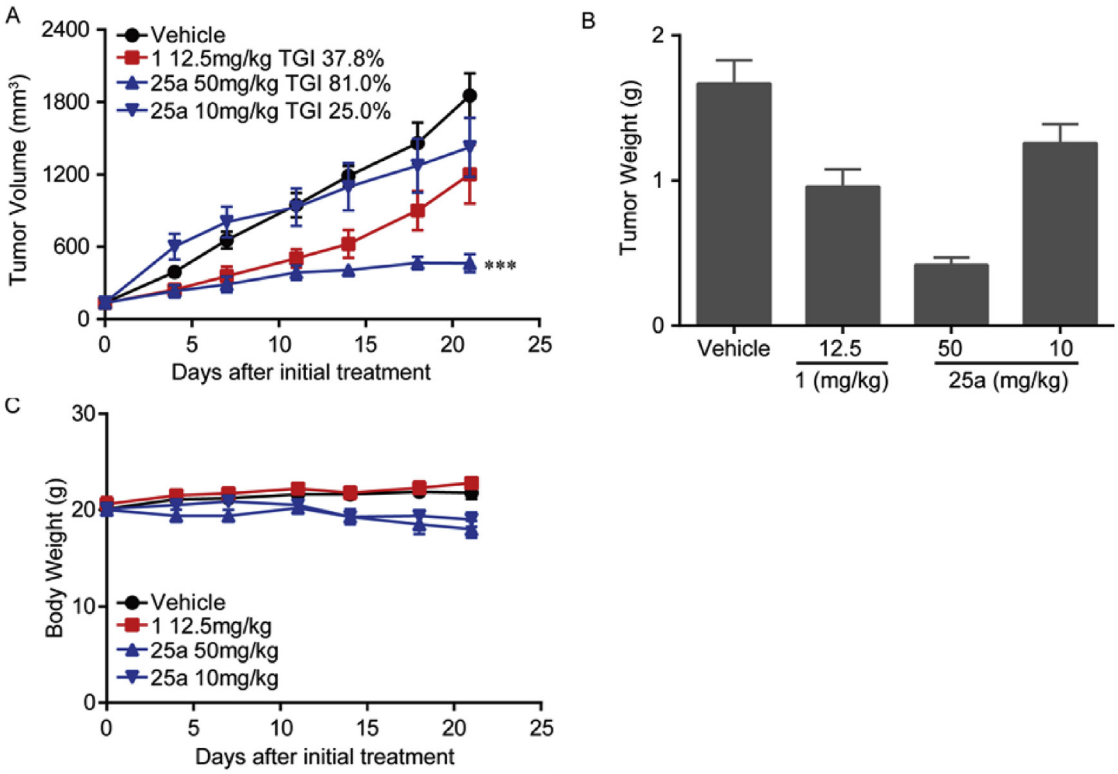

Fig. 4. The inhibitory effect of **25a** on tumor growth in SNU-16 xenograft model. Results are expressed as the mean ± SEM (n = 6 for the inhibitor-treated group, n = 12 for the vehicle control group). ***$p < 0.001$. vs vehicle group, as determined using a *t*-test.

removed under reduced pressure, and the residue was redissolved in DCM and was washed with saturated $NaHCO_3$ (aq) and brine, then dried over anhydrous Na_2SO_4, filtered and concentrated. The resulting residue was further purified via silica gel chromatography to give **23a** as a white solid (98 mg, 95%). ^{1}H NMR (300 MHz, $CDCl_3$) δ 9.06 (d, J = 9.4 Hz, 1H), 8.24 (dd, J = 12.0, 6.5 Hz, 2H), 7.98 (d, J = 8.1 Hz, 1H), 7.59–7.54 (m, 2H), 7.36 (d, J = 9.2 Hz, 1H), 6.91–6.81 (m, 2H), 4.02 (s, 3H).

24a was obtained according to the procedure of preparing **19a** using **23a** and **7a**. White solid; yield 52%; ^{1}H NMR (300 MHz, $CDCl_3$) δ 9.02 (d, J = 9.4 Hz, 1H), 8.58 (s, 1H), 8.16 (dd, J = 10.2, 6.5 Hz, 2H), 8.08 (d, J = 2.0 Hz, 1H), 7.96 (d, J = 8.2 Hz, 1H), 7.78 (d, J = 8.8 Hz, 2H), 7.58 (d, J = 2.3 Hz, 1H), 7.52 (t, J = 7.8 Hz, 1H), 7.42 (dd, J = 9.4, 2.4 Hz, 1H), 6.89 (d, J = 8.8 Hz, 2H), 6.66 (dd, J = 5.7, 2.1 Hz, 1H), 4.01 (s, 3H), 3.66 (d, J = 12.0 Hz, 2H), 3.03–2.97 (m, 2H), 2.40 (t, J = 11.3 Hz, 2H), 1.15 (d, J = 6.3 Hz, 6H). ^{13}C NMR (126 MHz, $CDCl_3$) δ 167.95, 166.35, 165.42, 153.98, 153.77, 152.26, 149.31, 135.15, 132.97, 130.00, 129.17, 129.01, 128.78, 127.37, 125.69, 122.92, 122.25, 117.71, 114.11, 109.01, 102.72, 54.48, 52.41, 50.59, 19.83. MS (ESI) *m/z* 511.30 $[M + H]^+$. HRMS: calcd for $C_{30}H_{31}N_4O_4$ $[M + H]^+$, 511.2340; found 511.2343.

*5.1.10. 7-(2-(4-((3R,5S)-3,5-dimethylpiperazin-1-yl)benzamido) pyridin-4-yloxy)-6-methoxy-N-methylquinoline-4-carboxamide (**24b**)*

7-(benzyloxy)-4-chloro-6-methoxyquinoline (200 mg, 0.70 mmol, 1 equiv), Zn $(CN)_2$ (165 mg, 1.40 mmol, 2equiv) and $Pd(PPh_3)_4$ (81 mg, 0.07 mmol, 0.1 equiv) were dissolved in DMF and the reaction mixture was heated at 160 °C overnight. The reaction mixture was then extracted with ethyl acetate and the organic phase was washed with saturated $NaHCO_3$ (aq) and brine, then dried over anhydrous Na_2SO_4, filtered and concentrated to give the crude product 7-(benzyloxy)-6-methoxyquinoline-4-carbonitrile for next step.

Crude 7-(benzyloxy)-6-methoxyquinoline-4-carbonitrile (183 mg, 0.63 mmol, 1 equiv) and NaOH (126 mg, 3.15 mmol, 5 equiv) were dissolved in EtOH: H_2O (1:1). The reaction mixture was refluxed for 6 h. Then the solvent was removed to minor amount under reduced pressure. The mixture was acidified with 2 N HCl (aq) to adjust PH to 5–6. The resulting precipitate was collected by filtration, washed with water and dried to a constant weight to afford 7-(benzyloxy)-6-methoxyquinoline-4-carboxylic acid. Then the crude acid obtained was dissolved in DCM, and methylamine hydrochloride (63.81 mg, 0.95 mmol, 1.5 equiv), EDCI (182 mg, 0.95 mmol, 1.5 equiv), HOBt (85 mg, 0.63 mmol, 1.0 equiv) and DIPEA (0.26 mL, 1.58 mmol, 2.5 equiv) were added successively. The reaction mixture was left to stir at room temperature overnight. The reaction mixture was then washed with saturated $NaHCO_3$ (aq) and brine, then dried over anhydrous Na_2SO_4, filtered and concentrated. The resulting residue was further purified via silica gel chromatography to give 7-(benzyloxy)-6-methoxy-N-methylquinoline-4-carboxamide (171 mg, 84%). ^{1}H NMR (300 MHz, $CDCl_3$) δ 8.66 (d, J = 4.5 Hz, 1H), 7.62 (s, 1H), 7.49 (d, J = 7.2 Hz, 2H), 7.44 (s, 1H), 7.40–7.29 (m, 3H), 7.23 (s, 1H), 6.21 (s, 1H), 5.30 (s, 2H), 4.00 (s, 3H), 3.09 (d, J = 4.9 Hz, 3H).

7-(benzyloxy)-6-methoxy-N-methylquinoline-4-carboxamide (171 mg, 0.53 mmol, 1 equiv), 10% Pd/C (20 mg) and potassium formate (134 mg, 1.59 mmol, 3 equiv) were dissolved in 17 mL MeOH and 10 mL H_2O. The reaction mixture was left to stir at room temperature overnight. The reaction mixture was then extracted with DCM and the organic phase was washed with saturated $NaHCO_3$ (aq) and brine, then dried over anhydrous Na_2SO_4, filtered and concentrated. The resulting residue was further purified via silica gel chromatography to give 7-hydroxy-6-methoxy-N-methylquinoline-4-carboxamide (107 mg, 87%). ^{1}H NMR (300 MHz, $CDCl_3$) δ 8.77 (d, J = 4.8 Hz, 1H), 7.49 (s, 1H), 7.32 (d, J = 4.3 Hz, 1H),

6.17 (s, 1H), 4.81 (s, 1H), 4.01 (s, 3H), 3.11 (d, $J = 4.8$ Hz, 3H).

2-chloro-4-nitropyridine (200 mg, 1.26 mmol, 1.2 equiv), 7-hydroxy-6-methoxy-N-methylquinoline-4-carboxamide (244 mg, 1.05 mmol, 1 equiv) and Cs_2CO_3 (684 mg, 2.10 mmol, 2 equiv) were dissolved in DMSO. The reaction mixture was left to stir at room temperature overnight. The mixture was diluted with ice water. The reaction mixture was then extracted with ethyl acetate and the organic phase was washed with saturated $NaHCO_3$ (aq) and brine, then dried over anhydrous Na_2SO_4, filtered and concentrated. The resulting residue was further purified via silica gel chromatography to give **23b** as light yellow solid (227 mg, 63%). ^{1}H NMR (300 MHz, $CDCl_3$) δ 8.84 (d, $J = 4.4$ Hz, 1H), 8.24 (d, $J = 6.2$ Hz, 1H), 7.83 (d, $J = 5.8$ Hz, 2H), 7.44 (d, $J = 4.4$ Hz, 1H), 6.82 (d, $J = 4.8$ Hz, 2H), 6.17 (s, 1H), 3.93 (s, 3H), 3.14 (d, $J = 4.9$ Hz, 3H).

24b was obtained according to the procedure of preparing **19a** using **7a** and **23b**. White solid; yield 59%; ^{1}H NMR (300 MHz, $CDCl_3$) δ 8.75 (d, $J = 4.4$ Hz, 1H), 8.67 (s, 1H), 8.15 (d, $J = 5.7$ Hz, 1H), 7.95 (d, $J = 2.1$ Hz, 1H), 7.83–7.70 (m, 4H), 7.36 (d, $J = 4.4$ Hz, 1H), 6.88 (d, $J = 8.8$ Hz, 2H), 6.71 (dd, $J = 5.7$, 2.3 Hz, 1H), 6.53 (d, $J = 4.6$ Hz, 1H), 3.93 (s, 3H), 3.72 (d, $J = 10.7$ Hz, 2H), 3.22 (s, 2H), 3.09 (d, $J = 4.8$ Hz, 3H), 2.80 (t, $J = 11.7$ Hz, 2H), 1.35 (d, $J = 6.3$ Hz, 6H). ^{13}C NMR (126 MHz, DMSO) δ 167.52, 165.85, 165.61, 154.79, 152.98, 151.59, 149.77, 149.02, 145.75, 144.81, 140.53, 130.04, 123.89, 122.94, 121.47, 119.93, 113.87, 108.24, 105.93, 101.42, 56.49, 52.07, 50.73, 26.66, 17.88. MS (ESI) m/z 541.34 $[M + H]^+$. HRMS: calcd for $C_{30}H_{33}N_6O_4$ $[M + H]^+$, 541.2558; found 541.2549.

5.1.11. 6-(2-(4-((3R,5S)-3,5-dimethylpiperazin-1-yl)benzamido) pyridin-4-yloxy)-N-ethyl-3,4-dihydroquinoline-1(2H)-carboxamide (**24c**)

23c was obtained according to the similar procedure of preparing **23b** starting from N-ethyl-6-hydroxy-3,4-dihydroquinoline-1(2H)-carboxamide. White solid, yield 40%; ^{1}H NMR (300 MHz, $CDCl_3$) δ 8.22 (d, $J = 5.5$ Hz, 1H), 7.40 (d, $J = 9.1$ Hz, 1H), 6.92–6.85 (m, 2H), 6.83–6.77 (m, 2H), 5.05 (s, 1H), 3.79–3.70 (m, 2H), 3.39–3.26 (m, 2H), 2.74 (t, $J = 6.7$ Hz, 2H), 1.94 (dt, $J = 12.8$, 6.6 Hz, 2H), 1.16 (t, $J = 7.2$ Hz, 3H).

24c was obtained according to the procedure of preparing **19a** using **23c** and **7a**. White solid; yield 57%; ^{1}H NMR (300 MHz, $CDCl_3$) δ 8.51 (s, 1H), 8.14 (d, $J = 5.6$ Hz, 1H), 7.98 (s, 1H), 7.79 (d, $J = 8.4$ Hz, 2H), 7.34 (d, $J = 8.2$ Hz, 1H), 6.93 (t, $J = 8.0$ Hz, 4H), 6.64 (d, $J = 5.7$ Hz, 1H), 5.10 (s, 1H), 3.77 (t, $J = 5.7$ Hz, 2H), 3.69 (d, $J = 12.0$ Hz, 2H), 3.39–3.26 (m, 2H), 3.05 (s, 2H), 2.76 (t, $J = 6.6$ Hz, 2H), 2.49 (s, 2H), 1.99–1.88 (m, 2H), 1.22–1.14 (m, 9H). ^{13}C NMR (126 MHz, $CDCl_3$) δ 166.60, 165.25, 156.68, 153.65, 153.42, 150.23, 149.03, 136.59, 134.06, 128.86, 124.70, 123.13, 121.34, 118.79, 114.23, 108.82, 101.97, 53.89, 50.74, 43.45, 35.78, 27.27, 23.60, 19.08, 15.35. MS (ESI) m/z 529.50 $[M + H]^+$. HRMS: calcd for $C_{30}H_{37}N_6O_3$ $[M + H]^+$, 529.2922; found 529.2931.

5.1.12. 4-((3R,5S)-3,5-dimethylpiperazin-1-yl)-N-(4-(5-(3-ethylureido)naphthalen-2-yloxy)pyridin-2-yl)benzamide (**24d**)

23d was obtained according to the similar procedure of preparing **23b** starting from 1-ethyl-3-(6-hydroxynaphthalen-1-yl) urea. White solid, yield 55%; ^{1}H NMR (300 MHz, $CDCl_3$) δ 8.21 (d, $J = 6.2$ Hz, 1H), 8.13 (d, $J = 9.1$ Hz, 1H), 7.81 (d, $J = 7.0$ Hz, 1H), 7.59 (s, 1H), 7.56–7.43 (m, 3H), 7.16 (dd, $J = 9.1$, 2.3 Hz, 1H), 6.82–6.80 (m, 2H), 3.28 (dd, $J = 12.7$, 6.7 Hz, 2H), 1.12 (t, $J = 7.3$ Hz, 3H).

24d was obtained according to the procedure of preparing **19a** using **23d** and **7a**. White solid; yield 65%; ^{1}H NMR (300 MHz, DMSO) δ 10.48 (s, 1H), 8.62 (s, 1H), 8.30–8.19 (m, 2H), 8.00 (d, $J = 7.4$ Hz, 1H), 7.88 (d, $J = 10.9$ Hz, 3H), 7.70 (s, 1H), 7.56 (d, $J = 8.0$ Hz, 1H), 7.45 (t, $J = 10.6$ Hz, 2H), 6.93 (d, $J = 8.6$ Hz, 2H), 6.83–6.76 (m, 1H), 6.61 (s, 1H), 3.76 (d, $J = 11.6$ Hz, 2H), 3.24–3.11 (m, 2H), 2.84 (s, 2H), 2.26 (t, $J = 10.9$ Hz, 2H), 1.11 (t, $J = 7.2$ Hz, 3H), 1.05 (d, $J = 6.0$ Hz, 6H). ^{13}C NMR (126 MHz, DMSO) δ 165.91, 165.85, 155.98, 154.89, 153.37, 151.79, 149.93, 136.13, 135.32, 130.01, 127.57, 124.94, 123.78, 122.45, 122.10, 120.24, 118.02, 116.72, 113.63, 108.98, 102.25, 53.27, 50.56, 34.57, 19.04, 15.89. MS (ESI) m/z 539.44 $[M + H]^+$. HRMS: calcd for $C_{31}H_{35}N_6O_3$ $[M + H]^+$, 539.2765; found 539.2776.

5.1.13. 4-((3R,5S)-3,5-dimethylpiperazin-1-yl)-N-(4-(4-(3-ethylureido)-2-methoxyphenoxy)pyridin-2-yl)benzamide (**24e**)

23e was obtained according to the similar procedure of preparing **23b** starting from 1-ethyl-3-(4-hydroxy-3-methoxyphenyl) urea. Grey solid; yield 71%. ^{1}H NMR (300 MHz, $CDCl_3$) δ 8.19 (d, $J = 6.1$ Hz, 1H), 7.43 (s, 1H), 6.99 (d, $J = 8.8$ Hz, 1H), 6.74 (s, 2H), 6.69 (d, $J = 8.8$ Hz, 1H), 6.37 (s, 1H), 4.67 (s, 1H), 3.79 (s, 3H), 3.34 (dd, $J = 15.8$, 8.6 Hz, 2H), 1.21 (t, $J = 7.2$ Hz, 3H).

24e was obtained according to the procedure of preparing **19a** using **23e** and **7a**. White solid; yield 55%; ^{1}H NMR (300 MHz, DMSO) δ 10.37 (s, 1H), 8.73 (s, 1H), 8.16 (d, $J = 5.6$ Hz, 1H), 7.90 (d, $J = 8.3$ Hz, 2H), 7.67 (s, 1H), 7.46 (s, 1H), 7.05–6.89 (m, 4H), 6.59 (d, $J = 5.6$ Hz, 1H), 6.23 (t, $J = 5.6$ Hz, 1H), 3.80 (d, $J = 11.4$ Hz, 2H), 3.69 (s, 3H), 3.17–3.07 (m, 2H), 2.90 (s, 2H), 2.33 (t, $J = 11.3$ Hz, 2H), 1.14–1.01 (m, 9H). ^{13}C NMR (126 MHz, DMSO) δ 166.65, 165.74, 155.62, 154.63, 153.39, 151.68, 149.34, 140.08, 135.46, 113.60, 110.14, 107.59, 103.53, 100.86, 55.96, 50.57, 34.42, 19.18, 15.96. MS (ESI) m/z 519.41 $[M + H]^+$. HRMS: calcd for $C_{28}H_{35}N_6O_4$ $[M + H]^+$, 519.2714; found 519.2725.

5.1.14. N-(4-(3,5-dimethoxyphenethoxy)pyridin-2-yl)-4-((3R,5S)-3,5-dimethylpiperazin-1-yl)benzamide (**24f**)

2,4-dichloropyridine (200 mg, 1.35 mmol, 1.1 equiv), 2-(3,5-dimethoxyphenyl)ethanol (224 mg, 1.23 mmol, 1 equiv) and t-BuOK (276 mg, 2.46 mmo, 2 equiv) were refluxed in t-BuOH overnight. The reaction mixture was filtered and concentrated under reduced pressure. The residue was redissolved in DCM and washed with brine, then dried over anhydrous Na_2SO_4, filtered and concentrated. The resulting residue was further purified via silica gel chromatography to give **23f** as white solid (257 mg, 71%). ^{1}H NMR (300 MHz, $CDCl_3$) δ 7.98 (d, $J = 5.5$ Hz, 1H), 6.85–6.77 (m, 1H), 6.69 (s, 1H), 6.38 (d, $J = 1.6$ Hz, 2H), 6.29 (s, 1H), 4.46 (t, $J = 7.0$ Hz, 2H), 3.72 (s, 6H), 2.96 (t, $J = 7.0$ Hz, 2H).

24f was obtained according to the similar procedure of preparing **19a** using **23f** and **7a**. White solid; yield 68%; ^{1}H NMR (300 MHz, $CDCl_3$) δ 8.05 (d, $J = 5.7$ Hz, 1H), 7.79–7.68 (m, 3H), 7.13 (dd, $J = 5.8$, 1.5 Hz, 1H), 7.10 (s, 1H), 6.91 (d, $J = 8.9$ Hz, 2H), 6.46 (d, $J = 2.0$ Hz, 2H), 6.33 (s, 1H), 4.51 (t, $J = 6.9$ Hz, 2H), 3.78 (s, 6H), 3.68 (d, $J = 10.2$ Hz, 2H), 3.03 (t, $J = 6.9$ Hz, 4H), 2.42 (t, $J = 11.2$ Hz, 2H), 1.16 (d, $J = 6.3$ Hz, 6H). ^{13}C NMR (126 MHz, $CDCl_3$) δ 165.65, 165.20, 160.90, 153.84, 147.74, 147.67, 141.12, 128.95, 123.00, 114.19, 108.47, 107.22, 99.85, 98.61, 66.64, 55.45, 54.48, 50.61, 36.03, 19.82. MS (ESI) m/z 491.30 $[M + H]^+$. HRMS: calcd for $C_{28}H_{35}N_4O_4$ $[M + H]^+$, 491.2653; found 491.2659.

5.1.15. N-(4-(2,6-dichloro-3,5-dimethoxyphenethoxy)pyridin-2-yl)-4-((3R,5S)-3,5-dimethylpiperazin-1-yl)benzamide (**24g**)

23g was obtained according to the similar procedure of preparing **23f** starting from 2-(2,6-dichloro-3,5-dimethoxyphenyl) ethanol. White solid, yield 66%. ^{1}H NMR (300 MHz, $CDCl_3$) δ 8.02 (d, $J = 5.5$ Hz, 1H), 6.85 (d, $J = 5.5$ Hz, 1H), 6.75 (s, 1H), 6.50 (s, 1H), 4.51 (t, $J = 7.1$ Hz, 2H), 3.91 (s, 6H), 3.48 (t, $J = 7.1$ Hz, 2H).

24g was obtained according to the similar procedure of preparing **19a** using **23g** and **7a**. White solid; yield 72%; ^{1}H NMR (300 MHz, $CDCl_3$) δ 8.04 (d, $J = 5.7$ Hz, 1H), 7.83 (s, 1H), 7.74 (d, $J = 8.7$ Hz, 2H), 7.20 (d, $J = 5.6$ Hz, 1H), 7.03 (s, 1H), 6.89 (d, $J = 8.7$ Hz, 2H), 6.48 (s, 1H), 4.49 (t, $J = 7.2$ Hz, 2H), 3.90 (s, 6H), 3.67 (d, $J = 10.7$ Hz, 2H), 3.49 (t, $J = 7.2$ Hz, 2H), 3.08–2.94 (m, 2H), 2.41 (t,

J = 11.2 Hz, 2H), 1.16 (d, J = 6.3 Hz, 6H). ^{13}C NMR (126 MHz, $CDCl_3$) δ 165.72, 165.11, 154.47, 153.79, 147.71, 136.21, 128.97, 122.98, 115.85, 114.13, 108.54, 99.82, 96.20, 63.79, 56.66, 54.47, 50.59, 31.59, 19.83. MS (ESI) m/z 559.20 $[M + H]^+$. HRMS: calcd for $C_{28}H_{33}Cl_2N_4O_4$ $[M + H]^+$, 559.1873; found 559.1882.

5.1.16. N-(5-(2,6-difluoro-3,5-dimethoxybenzyloxy)pyridin-2-yl)-4-((3R,5S)-3,5-dimethylpiperazin-1-yl)benzamide (**24h**)

6-chloropyridin-3-ol (356 mg, 2.76 mmol, 1.2 equiv), 2,6-difluoro-3,5-dimethoxybenzyl methanesulfonate (649 mg, 2.30 mmol, 1 equiv) and K_2CO_3 (795 mg, 5.75 mmol, 2 equiv) dissolved in DMF were heated at 60 °C overnight. The reaction mixture was then extracted with ethyl acetate and the organic phase was washed with saturated $NaHCO_3$ (aq) and brine, then dried over anhydrous Na_2SO_4, filtered and concentrated. The resulting residue was further purified via silica gel chromatography to give **23h** (759 mg, 65%). ^{1}H NMR (300 MHz, $CDCl_3$) δ 8.07 (d, J = 2.7 Hz, 1H), 7.25–7.16 (m, 2H), 6.62 (t, J = 8.1 Hz, 1H), 5.11 (s, 2H), 3.83 (s, 6H).

24h was obtained according to the similar procedure of preparing **19a** using **23h** and **7a**. White solid; yield 67%; ^{1}H NMR (300 MHz, $CDCl_3$) δ 8.47 (s, 1H), 8.33 (d, J = 9.1 Hz, 1H), 8.04 (s, 1H), 7.82 (d, J = 8.7 Hz, 2H), 7.41 (dd, J = 9.0, 2.6 Hz, 1H), 6.92 (d, J = 8.7 Hz, 2H), 6.67 (t, J = 8.1 Hz, 1H), 5.17 (s, 2H), 3.89 (s, 6H), 3.68 (d, J = 11.4 Hz, 2H), 3.01 (s, 2H), 2.41 (t, J = 11.2 Hz, 2H), 1.16 (d, J = 6.3 Hz, 6H). ^{13}C NMR (126 MHz, $CDCl_3$) δ 165.07, 153.66, 151.59, 146.41, 145.06 (dd, J = 244.2, 5.7 Hz), 143.69 (dd, J = 11.4, 3.8 Hz), 135.91, 128.90, 125.14, 123.34, 114.63, 114.22, 113.61 (t, J = 17.3 Hz), 101.98, 59.64, 57.44, 54.58, 50.60, 19.81. MS (ESI) m/z 513.30 $[M + H]^+$. HRMS: calcd for $C_{27}H_{31}F_2N_4O_4$ $[M + H]^+$, 513.2308; found 513.2309.

5.1.17. N-(5-(1-(3,5-dicholoropyridin-4-yl)ethoxy)pyridin-2-yl)-4-((3R,5S)-3,5-dimethylpiperazin-1-yl)benzamide (**24i**)

23i was obtained according to the similar procedure of preparing **23h** starting from 1-(3,5-dicholoropyridin-4-yl)ethyl methanesulfonate. White solid, yield 61%. ^{1}H NMR (300 MHz, $CDCl_3$) δ 8.44 (s, 1H), 7.97 (d, J = 2.4 Hz, 1H), 7.18–7.09 (m, 1H), 6.01–5.91 (m, 1H), 1.79 (d, J = 6.7 Hz, 3H).

24i was obtained according to the similar procedure of preparing **19a** using **23i** and **7a**. White solid; yield 61%; ^{1}H NMR (300 MHz, $CDCl_3$) δ 8.44 (s, 2H), 8.42 (s, 1H), 8.24 (d, J = 9.0 Hz, 1H), 7.91 (d, J = 2.2 Hz, 1H), 7.78 (d, J = 8.7 Hz, 2H), 7.23 (d, J = 9.3 Hz, 1H), 6.90 (d, J = 8.8 Hz, 2H), 5.98 (q, J = 6.4 Hz, 1H), 3.67 (d, J = 10.9 Hz, 2H), 3.08–2.97 (m, 2H), 2.43 (t, J = 11.2 Hz, 2H), 1.79 (d, J = 6.6 Hz, 3H), 1.17 (d, J = 6.3 Hz, 6H). ^{13}C NMR (126 MHz, $CDCl_3$) δ 164.98, 153.52, 150.00, 149.07, 146.40, 143.59, 135.62, 131.21, 128.87, 125.23, 123.42, 114.71, 114.37, 72.65, 54.26, 50.78, 29.84, 19.41, 18.78. MS (ESI) m/z 500.30 $[M + H]^+$. HRMS: calcd for $C_{25}H_{28}Cl_2N_5O_2$ $[M + H]^+$, 500.1615; found 500.1622.

5.1.18. N-Methyl-6-(2-(4-(4-methylpiperazin-1-yl)benzamido) pyridin-4-yloxy)-1-naphthamide (**25a**)

7e was obtained according to the similar procedure of preparing **7a** starting from ethyl 4-fluorobenzoate and 1-methylpiperazine. White solid; yield 54%; ^{1}H NMR (300 MHz, $CDCl_3$) δ 7.72 (d, J = 8.8 Hz, 2H), 6.89 (d, J = 8.8 Hz, 2H), 5.76 (s, 2H), 3.42–3.26 (m, 4H), 2.68–2.49 (m, 4H), 2.35 (s, 3H).

25a was obtained according to the similar procedure of preparing **19a** using **15** and **7e**. White solid; yield 70%; ^{1}H NMR (300 MHz, $CDCl_3$) δ 8.59 (s, 1H), 8.38 (d, J = 9.2 Hz, 1H), 8.13 (d, J = 5.6 Hz, 1H), 8.02 (s, 1H), 7.83 (d, J = 8.0 Hz, 1H), 7.75 (d, J = 8.3 Hz, 2H), 7.54 (d, J = 7.7 Hz, 2H), 7.44 (t, J = 7.6 Hz, 1H), 7.33 (d, J = 9.1 Hz, 1H), 6.88 (d, J = 8.4 Hz, 2H), 6.65 (d, J = 5.6 Hz, 1H), 6.28 (d, J = 3.9 Hz, 1H), 3.34 (s, 4H), 3.05 (d, J = 4.6 Hz, 3H), 2.56 (s, 4H), 2.35 (s, 3H). ^{13}C NMR (126 MHz, $CDCl_3$) δ 169.93, 166.18, 165.16, 153.56, 153.49, 152.03, 148.99, 134.61, 134.58, 129.80, 128.66, 128.12, 127.73, 125.62, 124.41, 122.89, 121.32, 117.42, 113.87, 108.79, 102.16, 54.52, 47.19, 45.87, 26.68. MS (ESI) m/z 496.30 $[M + H]^+$. HRMS: calcd for $C_{29}H_{30}N_5O_3$ $[M + H]^+$, 496.2343; found 496.2355.

5.1.19. N-Methyl-6-(2-(4-morpholinobenzamido)pyridin-4-yloxy)-1-naphthamide (**25b**)

7f was obtained according to the similar procedure of preparing **7a** starting from ethyl 4-fluorobenzoate and morpholine. White solid; yield 60%; ^{1}H NMR (300 MHz, DMSO) δ 7.76 (d, J = 8.9 Hz, 2H), 7.70 (s, 1H), 7.04 (s, 1H), 6.94 (d, J = 8.9 Hz, 2H), 3.79–3.66 (m, 4H), 3.25–3.15 (m, 4H).

25b was obtained according to the similar procedure of preparing **19a** using **15** and **7f**. White solid; yield 74%; ^{1}H NMR (300 MHz, $CDCl_3$) δ 8.51 (s, 1H), 8.41 (d, J = 9.2 Hz, 1H), 8.16 (d, J = 5.7 Hz, 1H), 8.04 (s, 1H), 7.83 (dd, J = 19.0, 8.2 Hz, 3H), 7.58 (d, J = 6.8 Hz, 2H), 7.48 (t, J = 7.7 Hz, 1H), 7.36 (d, J = 9.1 Hz, 1H), 6.90 (d, J = 8.4 Hz, 2H), 6.67 (d, J = 5.8 Hz, 1H), 6.09 (s, 1H), 3.90–3.80 (m, 4H), 3.33–3.24 (m, 4H), 3.10 (d, J = 4.7 Hz, 3H). ^{13}C NMR (126 MHz, $CDCl_3$) δ 170.22, 166.55, 165.39, 153.99, 153.81, 152.38, 149.30, 134.94, 130.19, 128.99, 128.45, 128.08, 125.95, 124.70, 123.80, 121.68, 117.76, 114.04, 109.16, 102.50, 66.75, 47.87, 27.04. MS (ESI) m/z 483.30 $[M + H]^+$. HRMS: calcd for $C_{28}H_{27}N_4O_4$ $[M + H]^+$, 483.2027; found 483.2024.

5.1.20. 6-(2-(4-(2,6-dimethylmorpholino)benzamido)pyridin-4-yloxy)-N-methyl-1-naphthamide (**25c**)

7g was obtained according to the similar procedure of preparing **7a** starting from ethyl 4-fluorobenzoate and 2,6-dimethylmorpholine. White solid; yield 55%; ^{1}H NMR (300 MHz, $CDCl_3$) δ 7.67 (d, J = 8.7 Hz, 2H), 6.82 (d, J = 8.7 Hz, 2H), 5.68 (s, 2H), 3.82–3.64 (m, 2H), 3.52 (d, J = 11.6 Hz, 2H), 2.44 (t, J = 11.4 Hz, 2H), 1.21 (d, J = 6.3 Hz, 6H).

25c was obtained according to the similar procedure of preparing **19a** using **15** and **7g**. White solid; yield 61%; ^{1}H NMR (300 MHz, $CDCl_3$) δ 8.48 (s, 1H), 8.41 (d, J = 9.2 Hz, 1H), 8.16 (d, J = 5.8 Hz, 1H), 8.04 (d, J = 1.6 Hz, 1H), 7.86 (d, J = 8.3 Hz, 1H), 7.78 (d, J = 8.8 Hz, 2H), 7.58 (d, J = 7.0 Hz, 2H), 7.52–7.44 (m, 1H), 7.36 (dd, J = 9.2, 2.0 Hz, 1H), 6.89 (d, J = 8.7 Hz, 2H), 6.67 (dd, J = 5.7, 1.8 Hz, 1H), 6.07 (d, J = 5.5 Hz, 1H), 3.83–3.71 (m, 2H), 3.59 (d, J = 11.4 Hz, 2H), 3.11 (d, J = 4.8 Hz, 3H), 2.52 (t, J = 11.3 Hz, 2H), 1.28 (d, J = 6.2 Hz, 6H). ^{13}C NMR (126 MHz, $CDCl_3$) δ 170.24, 166.54, 165.42, 153.84, 153.60, 152.34, 149.26, 134.91, 130.16, 129.17, 129.00, 128.44, 128.06, 125.94, 124.71, 123.34, 121.66, 117.76, 113.98, 109.13, 102.46, 71.57, 53.15, 27.01, 19.16. MS (ESI) m/z 511.50 $[M + H]^+$. HRMS: calcd for $C_{30}H_{31}N_4O_4$ $[M + H]^+$, 511.2340; found 511.2337.

5.1.21. N-Methyl-6-(2-(4-(3-methylpiperazin-1-yl)benzamido) pyridin-4-yloxy)-1-naphthamide (**25d**)

7h was obtained according to the similar procedure of preparing **7a** starting from ethyl 4-fluorobenzoate and 2-methylpiperazine. White solid; yield 43%; ^{1}H NMR (300 MHz, $CDCl_3$) δ 7.72 (d, J = 8.5 Hz, 2H), 6.83 (d, J = 8.5 Hz, 2H), 5.81 (s, 2H), 4.33 (s, 1H), 3.93 (d, J = 13.0 Hz, 1H), 3.64 (d, J = 12.3 Hz, 1H), 3.51 (d, J = 12.4 Hz, 1H), 3.34–3.23 (m, 1H), 3.12 (dd, J = 12.5, 3.7 Hz, 1H), 2.92 (td, J = 11.9, 3.8 Hz, 1H), 1.48 (s, 9H), 1.24 (s, 3H).

25d was obtained according to the similar procedure of preparing **19a** using **15** and **7h**. White solid; yield 49%; ^{1}H NMR (300 MHz, DMSO) δ 10.50 (s, 1H), 8.53 (d, J = 4.7 Hz, 1H), 8.34 (d, J = 9.4 Hz, 1H), 8.28 (d, J = 5.6 Hz, 1H), 8.02 (dd, J = 6.9, 1.9 Hz, 1H), 7.90 (s, 1H), 7.88–7.83 (m, 2H), 7.81 (d, J = 2.0 Hz, 1H), 7.65–7.54 (m, 2H), 7.45 (dd, J = 9.2, 2.3 Hz, 1H), 6.94 (d, J = 9.1 Hz, 2H), 6.81 (dd, J = 5.8, 2.1 Hz, 1H), 3.74 (t, J = 10.2 Hz, 2H), 3.01 (d, J = 10.6 Hz, 1H), 2.86 (s, 3H), 2.84–2.64 (m, 3H), 2.42–2.32 (m, 1H), 1.06 (d, J = 6.3 Hz, 3H). ^{13}C NMR (126 MHz, DMSO) δ 169.29, 165.90, 165.79,

154.94, 153.73, 152.02, 149.97, 135.44, 134.76, 130.00, 129.86, 128.82, 127.95, 126.52, 125.28, 122.53, 121.69, 117.88, 113.61, 109.05, 102.31, 54.14, 50.49, 47.00, 45.17, 26.66, 19.28. MS (ESI) *m/z* 496.30 [M + H]$^+$. HRMS: calcd for $C_{29}H_{30}N_5O_3$ [M + H]$^+$, 496.2343; found 496.2336.

*5.1.22. 6-(2-(4-(4-(2-hydroxyethyl)piperazin-1-yl)benzamido) pyridin-4-yloxy)-N-methyl-1-naphthamide (**25e**)*

7i was obtained according to the similar procedure of preparing **7a** starting from ethyl 4-fluorobenzoate and 2-(piperazin-1-yl) ethanol. White solid; yield 48%; ^{1}H NMR (300 MHz, DMSO) δ 7.73 (d, *J* = 8.7 Hz, 2H), 7.69 (s, 1H), 7.01 (s, 1H), 6.92 (d, *J* = 8.5 Hz, 2H), 4.44 (t, *J* = 5.5 Hz, 1H), 3.53 (q, *J* = 5.9 Hz, 2H), 3.23 (s, 3H), 2.53 (s, 3H), 2.43 (t, *J* = 6.1 Hz, 2H).

25e was obtained according to the similar procedure of preparing **19a** using **15** and **7i**. White solid; yield 51%; ^{1}H NMR (300 MHz, $CDCl_3$) δ 8.46 (s, 1H), 8.34 (d, *J* = 9.2 Hz, 1H), 8.10 (d, *J* = 5.7 Hz, 1H), 7.98 (d, *J* = 2.0 Hz, 1H), 7.80 (d, *J* = 8.8 Hz, 1H), 7.72 (d, *J* = 8.8 Hz, 2H), 7.52 (d, *J* = 6.7 Hz, 2H), 7.45–7.39 (m, 1H), 7.29 (dd, *J* = 9.4, 2.2 Hz, 1H), 6.84 (d, *J* = 8.9 Hz, 2H), 6.61 (dd, *J* = 5.5, 2.0 Hz, 1H), 6.04 (d, *J* = 2.0 Hz, 1H), 3.62 (t, *J* = 5.1 Hz, 2H), 3.35–3.25 (m, 4H), 3.04 (d, *J* = 4.9 Hz, 3H), 2.65–2.59 (m, 4H), 2.58–2.53 (m, 2H). ^{13}C NMR (126 MHz, $CDCl_3$) δ 170.71, 166.77, 165.84, 153.79, 153.73, 152.04, 148.99, 134.79, 134.75, 130.09, 128.99, 128.23, 127.98, 125.97, 124.93, 122.98, 121.58, 117.88, 114.21, 109.11, 102.38, 59.86, 58.14, 52.87, 47.44, 26.76. MS (ESI) *m/z* 526.30 [M + H]$^+$. HRMS: calcd for $C_{30}H_{32}N_5O_4$ [M + H]$^+$, 526.2449; found 526.2460.

*5.1.23. N-Methyl-6-(2-(4-(piperazin-1-yl)benzamido)pyridin-4-yloxy)-1-naphthamide (**27**)*

26 was obtained according to the similar procedure of preparing **7a** starting from *tert*-butyl 4-(4-(ethoxycarbonyl)phenyl)piperidine-1-carboxylate [42]. White solid; yield 54%; ^{1}H NMR (300 MHz, $CDCl_3$) δ 7.70 (d, *J* = 8.1 Hz, 2H), 7.22 (d, *J* = 9.2 Hz, 2H), 5.97 (s, 1H), 5.64 (s, 1H), 4.20 (d, *J* = 10.0 Hz, 2H), 2.84–2.57 (m, 3H), 1.77 (d, *J* = 12.8 Hz, 2H), 1.65–1.58 (m, 1H), 1.55 (d, *J* = 4.5 Hz, 1H), 1.42 (s, 9H).

27 was obtained according to the similar procedure of preparing **19a** using **15** and **26**. White solid; yield 52%; ^{1}H NMR (300 MHz, DMSO) δ 10.83 (s, 1H), 8.55 (d, *J* = 4.7 Hz, 1H), 8.33 (dd, *J* = 10.3, 7.5 Hz, 2H), 8.03 (dd, *J* = 7.2, 1.9 Hz, 1H), 7.95 (d, *J* = 8.2 Hz, 2H), 7.86 (d, *J* = 2.1 Hz, 1H), 7.82 (d, *J* = 2.2 Hz, 1H), 7.64–7.55 (m, 2H), 7.46 (dd, *J* = 9.2, 2.4 Hz, 1H), 7.33 (d, *J* = 8.2 Hz, 2H), 6.85 (dd, *J* = 5.7, 2.2 Hz, 1H), 3.36 (s, 2H), 3.04–2.89 (m, 3H), 2.86 (d, *J* = 4.5 Hz, 3H), 1.96–1.77 (m, 4H). ^{13}C NMR (126 MHz, DMSO) δ 169.28, 166.29, 165.89, 154.58, 151.96, 150.12, 149.42, 135.41, 134.76, 132.59, 129.88, 128.86, 127.99, 127.00, 126.54, 125.34, 121.68, 117.94, 109.44, 102.53, 43.90, 39.41, 29.61, 26.66. MS (ESI) *m/z* 481.30 [M + H]$^+$. HRMS: calcd for $C_{29}H_{29}N_4O_3$ [M + H]$^+$, 481.2234; found 481.2247.

*5.1.24. 6-(2-(4-(1-(2-hydroxyethyl)piperidin-4-yl)benzamido) pyridin-4-yloxy)-N-methyl-1-naphthamide (**28**)*

27 (52 mg, 0.11 mmol, 1 equiv), 2-bromoethanol (24 μL, 0.33 mmol, 3 equiv) and K_2CO_3 (30 mg, 0.22 mmol, 2 equiv) were heated at 80 °C in DMF for 5 h. The reaction mixture was then extracted with ethyl acetate and the organic phase was washed with saturated $NaHCO_3$ (aq) and brine, then dried over anhydrous Na_2SO_4, filtered and concentrated. The resulting residue was further purified via silica gel chromatography to give **28** as white solid (35 mg, 62%). ^{1}H NMR (300 MHz, DMSO) δ 10.78 (s, 1H), 8.53 (d, *J* = 4.5 Hz, 1H), 8.32 (dd, *J* = 11.0, 7.5 Hz, 2H), 8.03 (dd, *J* = 7.0, 2.1 Hz, 1H), 7.91 (d, *J* = 8.2 Hz, 2H), 7.86 (d, *J* = 2.0 Hz, 1H), 7.81 (d, *J* = 2.1 Hz, 1H), 7.65–7.55 (m, 2H), 7.46 (dd, *J* = 9.3, 2.4 Hz, 1H), 7.34 (d, *J* = 8.2 Hz, 2H), 6.84 (dd, *J* = 5.7, 2.3 Hz, 1H), 3.56 (s, 2H), 3.08 (s, 2H), 2.86 (d, *J* = 3.4 Hz, 3H), 2.59 (s, 2H), 2.27 (s, 3H), 1.77 (s, 4H). ^{13}C NMR (126 MHz, DMSO) δ 169.27, 166.38, 165.87, 154.61, 151.99, 150.66, 150.10, 135.43, 134.76, 132.22, 129.87, 128.85, 128.69, 127.98, 127.13, 126.54, 125.31, 121.67, 117.91, 109.41, 102.52, 60.48, 58.40, 54.16, 41.57, 32.47, 26.66. MS (ESI) *m/z* 525.40 [M + H]$^+$. HRMS: calcd for $C_{31}H_{33}N_4O_4$ [M + H]$^+$, 525.2496; found 525.2490.

*5.1.25. 6-(2-(4-((4-hydroxytetrahydro-2H-pyran-4-yl) methylamino)benzamido)pyridin-4-yloxy)-N-methyl-1-naphthamide (**30a**)*

4-nitrobenzamide (166 mg, 1.00 mmol, 1 equiv) and **15** (406 mg, 1.3 mmol, 1.3 equiv) were dissolved in 10 mL dry dioxane. Then $Pd_2(dba)_3$ (92 mg, 0.10 mmol, 0.1 equiv), Xantphos (116 mg, 0.20 mmol, 0.2 equiv) and Cs_2CO_3 (652 mg, 2.00 mmol, 2 equiv) were added to the mixture above. Then the reaction mixture was left to stir at 110 °C for 5 h under nitrogen atmosphere. The reaction mixture was then extracted with DCM and the organic phase was washed with saturated $NaHCO_3$ (aq) and brine, then dried over anhydrous Na_2SO_4, filtered and concentrated. The resulting residue was further purified via silica gel chromatography to give N-methyl-6-(2-(4-nitrobenzamido)pyridin-4-yloxy)-1-naphthamide as light yellow solid (340 mg, 76.8%). ^{1}H NMR (300 MHz, DMSO) δ 11.28 (s, 1H), 8.52 (d, *J* = 3.1 Hz, 1H), 8.38–8.24 (m, 4H), 8.16 (d, *J* = 8.7 Hz, 2H), 8.03 (d, *J* = 6.9 Hz, 1H), 7.83 (d, *J* = 5.9 Hz, 2H), 7.60 (d, *J* = 6.9 Hz, 2H), 7.46 (d, *J* = 10.0 Hz, 1H), 6.88 (d, *J* = 5.6 Hz, 1H), 2.86 (d, *J* = 4.4 Hz, 3H).

N-methyl-6-(2-(4-nitrobenzamido)pyridin-4-yloxy)-1-naphthamide (340 mg, 0.77 mmol, 1 equiv), Zn (251 mg, 3.84 mmol, 5 equiv) and NH_4Cl (82 mg, 1.54 mmol, 2 equiv) were dissolved in 15 mL MeOH and 15 mL THF. The reaction mixture was left to stir at room temperature overnight. After completion, the mixture was filtered and the filtrate was concentrated and further purified via silica gel chromatography to give **29** as white solid (233 mg, 73.5%). ^{1}H NMR (300 MHz, $CDCl_3$) δ 8.47 (s, 1H), 8.40 (d, *J* = 9.7 Hz, 1H), 8.15 (d, *J* = 5.9 Hz, 1H), 8.03 (s, 1H), 7.85 (d, *J* = 8.6 Hz, 1H), 7.70 (d, *J* = 7.6 Hz, 2H), 7.58 (d, *J* = 7.8 Hz, 2H), 7.47 (t, *J* = 7.9 Hz, 1H), 7.35 (d, *J* = 8.5 Hz, 1H), 6.68 (d, *J* = 7.7 Hz, 3H), 6.06 (s, 1H), 4.05 (s, 2H), 3.10 (d, *J* = 4.3 Hz, 3H).

29 (82 mg, 0.20 mmol, 1 equiv), 1,6-dioxaspiro[2.5]octane (67 mg, 0.60 mmol, 3 equiv) and DIPEA (0.17 mL, 1.00 mmol, 5 equiv) were heated at 75 °C in EtOH for 4 d. The solvent was removed under reduced pressure, and the residue was redissolved in DCM. The mixture was washed with saturated NH_4Cl (aq) and brine, then dried over anhydrous Na_2SO_4, filtered and concentrated. The resulting residue was further purified via silica gel chromatography to give **30a** as white solid (34 mg, 32%). ^{1}H NMR (300 MHz, DMSO) δ 10.29 (s, 1H), 8.53 (d, *J* = 5.3 Hz, 1H), 8.33 (d, *J* = 9.2 Hz, 1H), 8.26 (d, *J* = 5.8 Hz, 1H), 8.02 (d, *J* = 7.6 Hz, 1H), 7.79 (dd, *J* = 16.6, 10.5 Hz, 3H), 7.64–7.53 (m, 2H), 7.45 (d, *J* = 9.1 Hz, 1H), 6.78 (d, *J* = 5.0 Hz, 1H), 6.66 (d, *J* = 8.2 Hz, 2H), 6.18 (t, *J* = 5.6 Hz, 1H), 4.54 (s, 1H), 3.61 (d, *J* = 6.8 Hz, 4H), 3.07 (d, *J* = 5.6 Hz, 2H), 2.86 (d, *J* = 4.1 Hz, 3H), 1.64–1.54 (m, 2H), 1.49–1.40 (m, 2H). ^{13}C NMR (126 MHz, DMSO) δ 169.29, 166.02, 165.73, 155.10, 153.25, 152.05, 149.92, 135.44, 134.75, 130.10, 129.85, 128.79, 127.93, 126.51, 125.26, 121.70, 119.97, 117.85, 111.38, 108.85, 102.16, 68.62, 63.31, 53.62, 35.61, 26.65. MS (ESI) *m/z* 527.30 [M + H]$^+$. HRMS: calcd for $C_{30}H_{31}N_4O_5$ [M + H]$^+$, 527.2289; found 527.2294.

*5.1.26. 6-(2-(4-acrylamidobenzamido)pyridin-4-yloxy)-N-methyl-1-naphthamide (**30b**)*

29 (94 mg, 0.23 mmol, 1 equiv) and DIPEA (76 μL, 0.46 mmol, 2 equiv) were dissolved in dry DCM and allowed to cool down to 0 °C. Acryloyl chloride (24 μL, 0.30 mmol, 1.3 equiv) was added dropwise. The reaction mixture was left to stir at room temperature overnight. The mixture was washed with saturated NH_4Cl (aq) and brine, then dried over anhydrous Na_2SO_4, filtered and concentrated.

The resulting residue was further purified via silica gel chromatography to give **30b** as white solid (86 mg, 80%). ^{1}H NMR (300 MHz, DMSO) δ 10.76 (s, 1H), 10.41 (s, 1H), 8.53 (d, J = 4.0 Hz, 1H), 8.41–8.25 (m, 2H), 8.03 (dd, J = 6.6, 2.5 Hz, 1H), 7.97 (d, J = 8.5 Hz, 2H), 7.83 (dd, J = 8.8, 2.3 Hz, 2H), 7.75 (d, J = 8.3 Hz, 2H), 7.65–7.55 (m, 2H), 7.46 (dd, J = 8.8, 1.6 Hz, 1H), 6.84 (d, J = 5.6 Hz, 1H), 6.46 (dd, J = 17.4, 9.9 Hz, 1H), 6.29 (d, J = 16.3 Hz, 1H), 5.81 (d, J = 10.7 Hz, 1H), 2.86 (s, 3H). ^{13}C NMR (126 MHz, DMSO) δ 169.28, 165.88, 163.97, 154.64, 151.96, 150.01, 142.84, 135.44, 134.76, 132.05, 129.87, 129.56, 128.85, 128.14, 127.98, 126.54, 125.31, 121.69, 118.92, 117.94, 109.36, 102.46, 26.66. MS (ESI) m/z 467.30 $[M + H]^+$. HRMS: calcd for $C_{27}H_{22}N_4NaO_4$ $[M + Na]^+$, 489.1533; found 489.1535.

5.1.27. N-methyl-6-(2-(4-(2-(pyrrolidin-1-yl)ethoxy)benzamido) pyridin-4-yloxy)-1-naphthamide (**33a**)

4-hydroxybenzamide (4.80 g, 35 mmol, 1 equiv), 1,2-dibromoethane (18 mL, 210 mmol, 6 equiv) and K_2CO_3 (5.33 g, 38.5 mmol, 1.1 equiv) were heated at 50 °C in acetone under nirtogen atomasphere. After completion, the mixture was filtered and the filtrate was concentrated and further purified via silica gel chromatography to give 4-(2-bromoethoxy)benzamide (4.36 g, 51%). ^{1}H NMR (300 MHz, $CDCl_3$) δ 7.79 (d, J = 7.7 Hz, 2H), 6.95 (d, J = 7.8 Hz, 2H), 5.74 (s, 2H), 4.35 (t, J = 6.1 Hz, 2H), 3.66 (t, J = 6.2 Hz, 2H).

4-(2-bromoethoxy)benzamide (1.00 g, 4.10 mmol, 1 equiv), pyrrolidine (321 mg, 4.51 mmol, 1.10 equiv) and K_2CO_3 (1.13 g, 8.20 mmol, 2 equiv) were refluxed in CH_3CN overnight. After completion, the mixture was filtered and the filtrate was concentrated and further purified via silica gel chromatography to give **32a** as white solid (595 mg, 62%). ^{1}H NMR (300 MHz, $CDCl_3$) δ 7.76 (d, J = 8.8 Hz, 2H), 6.93 (d, J = 8.8 Hz, 2H), 6.00 (s, 2H), 4.14 (t, J = 5.9 Hz, 2H), 2.91 (t, J = 5.9 Hz, 2H), 2.63 (s, 4H), 1.80 (dt, J = 6.5, 3.2 Hz, 4H).

33a was obtained according to the similar procedure of preparing **19a** using **15** and **32a**. White solid; yield 67%; ^{1}H NMR (300 MHz, $CDCl_3$) δ 8.56 (s, 1H), 8.41 (d, J = 9.2 Hz, 1H), 8.15 (d, J = 5.7 Hz, 1H), 8.03 (d, J = 1.9 Hz, 1H), 7.84 (t, J = 9.4 Hz, 3H), 7.58 (d, J = 6.0 Hz, 2H), 7.52–7.44 (m, 1H), 7.35 (dd, J = 9.2, 2.3 Hz, 1H), 6.97 (d, J = 8.7 Hz, 2H), 6.67 (dd, J = 5.7, 2.1 Hz, 1H), 6.13 (d, J = 3.6 Hz, 1H), 4.16 (t, J = 5.8 Hz, 2H), 3.10 (d, J = 4.9 Hz, 3H), 2.92 (t, J = 5.8 Hz, 2H), 2.64 (s, 4H), 1.82 (s, 4H). ^{13}C NMR (126 MHz, $CDCl_3$) δ 170.19, 166.51, 165.36, 162.26, 153.66, 152.33, 149.33, 134.90, 130.16, 129.25, 128.43, 128.05, 126.32, 125.92, 124.67, 121.63, 117.72, 114.73, 109.22, 102.55, 67.40, 54.98, 54.87, 27.00, 23.62. MS (ESI) m/z 511.30 $[M + H]^+$. HRMS: calcd for $C_{30}H_{31}N_4O_4$ $[M + H]^+$, 511.2340; found 511.2332.

5.1.28. 6-(2-(4-(2-(3,3-difluoroazetidin-1-yl)ethoxy)benzamido) pyridin-4-yloxy)-N-methyl-1-naphthamide (**33b**)

32b was obtained according to the similar procedure of preparing **32a** using 3,3-difluoroazetidine hydrochloride. White solid; yield 55%; ^{1}H NMR (300 MHz, $CDCl_3$) δ 7.77 (d, J = 8.7 Hz, 2H), 6.92 (d, J = 8.7 Hz, 2H), 5.78 (s, 2H), 4.09 (t, J = 5.1 Hz, 2H), 3.73 (t, J = 12.0 Hz, 4H), 3.00 (t, J = 5.0 Hz, 2H).

33b was obtained according to the similar procedure of preparing **19a** using **15** and **32b**. White solid; yield 63%; ^{1}H NMR (300 MHz, $CDCl_3$) δ 8.60 (s, 1H), 8.40 (d, J = 9.2 Hz, 1H), 8.14 (d, J = 5.7 Hz, 1H), 8.03 (s, 1H), 7.83 (t, J = 8.6 Hz, 3H), 7.62–7.53 (m, 2H), 7.46 (t, J = 7.6 Hz, 1H), 7.34 (dd, J = 9.3, 2.0 Hz, 1H), 6.92 (d, J = 8.6 Hz, 2H), 6.67 (dd, J = 5.5, 1.8 Hz, 1H), 6.15 (d, J = 4.5 Hz, 1H), 4.08 (t, J = 5.0 Hz, 2H), 3.73 (t, J = 12.0 Hz, 4H), 3.08 (d, J = 4.8 Hz, 3H), 2.99 (t, J = 4.7 Hz, 2H). ^{13}C NMR (126 MHz, $CDCl_3$) δ 170.31, 166.67, 165.42, 162.06, 153.76, 152.45, 149.46, 135.04, 130.30, 129.46, 128.60, 128.21, 126.79, 126.07, 124.82, 121.76, 117.87, 116.95 (t, J = 275.9 Hz), 114.71, 109.39, 102.73, 67.74, 66.02, (t, J = 22.7 Hz), 57.46, 27.14. MS (ESI) m/z 555.30 $[M + Na]^+$. HRMS: calcd for $C_{29}H_{26}F_2N_4NaO_4$ $[M + Na]^+$, 555.1814; found 555.1824.

5.1.29. 6-(2-(4-(2-(3-fluoroazetidin-1-yl)ethoxy)benzamido) pyridin-4-yloxy)-N-methyl-1-naphthamide (**33c**)

32c was obtained according to the similar procedure of preparing **32a** using 3-fluoroazetidine hydrochloride. White solid; yield 59%; ^{1}H NMR (300 MHz, $CDCl_3$) δ 7.77 (d, J = 8.6 Hz, 2H), 6.92 (d, J = 8.6 Hz, 2H), 5.77 (s, 2H), 5.28–5.21 (m, 0.5H), 5.09–5.02 (m, 0.5H), 4.04 (t, J = 5.2 Hz, 2H), 3.85–3.73 (m, 2H), 3.38–3.21 (m, 2H), 2.93 (t, J = 5.2 Hz, 2H).

33c was obtained according to the similar procedure of preparing **19a** using **15** and **32c**. White solid; yield 57%; ^{1}H NMR (300 MHz, $CDCl_3$) δ 8.59 (s, 1H), 8.40 (d, J = 9.2 Hz, 1H), 8.14 (d, J = 5.7 Hz, 1H), 8.03 (s, 1H), 7.91–7.77 (m, 3H), 7.61–7.53 (m, 2H), 7.46 (t, J = 7.6 Hz, 1H), 7.34 (dd, J = 9.1, 2.1 Hz, 1H), 6.93 (d, J = 8.7 Hz, 2H), 6.66 (dd, J = 5.6, 2.0 Hz, 1H), 6.16 (d, J = 4.5 Hz, 1H), 5.28–5.19 (m, 1H), 5.09–5.00 (m, 1H), 4.04 (t, J = 5.2 Hz, 2H), 3.85–3.72 (m, 2H), 3.33 (dd, J = 8.2, 6.0 Hz, 1H), 3.25 (dd, J = 8.2, 6.1 Hz, 1H), 3.08 (d, J = 4.8 Hz, 3H), 2.93 (t, J = 5.1 Hz, 2H). ^{13}C NMR (126 MHz, $CDCl_3$) δ 170.22, 166.54, 165.39, 162.11, 153.69, 152.33, 149.36, 134.92, 130.17, 129.32, 128.47, 128.08, 126.53, 125.96, 124.72, 121.63, 117.75, 114.63, 109.25, 102.61, 82.66 (d, J = 205.4 Hz), 67.17, 62.71(d, J = 20.2 Hz), 58.19, 27.02. MS (ESI) m/z 515.30 $[M + H]^+$. HRMS: calcd for $C_{29}H_{27}FN_4NaO_4$ $[M + Na]^+$, 537.1909; found 537.1917.

5.1.30. 6-(2-(4-((1-aminocyclopropyl)methoxy)benzamido) pyridin-4-yloxy)-N-methyl-1-naphthamide (**33d**)

Ethyl 4-hydroxybenzoate (322 mg, 1.50 mmol, 1 equiv), *tert*-butyl 1-(iodomethyl)cyclopropylcarbamate (668 mg, 2.25 mmol, 1.5 equiv) and K_2CO_3 (621 mg, 4.50 mmol, 3 equiv) in acetone were refluxed overnight. After completion, the mixture was filtered and the filtrate was concentrated and further purified via silica gel chromatography to give compound **31** (322 mg, 64%). ^{1}H NMR (300 MHz, $CDCl_3$) δ 7.92 (d, J = 8.7 Hz, 2H), 6.84 (d, J = 8.7 Hz, 2H), 4.28 (q, J = 7.1 Hz, 2H), 3.96 (s, 2H), 1.37 (s, 9H), 1.32 (t, J = 7.2 Hz, 3H), 0.86 (d, J = 8.4 Hz, 4H).

32d was obtained according to the similar procedure of preparing **7a** starting from **31**. White solid; yield 51%; ^{1}H NMR (300 MHz, DMSO) δ 7.81 (d, J = 8.7 Hz, 3H), 7.30 (s, 1H), 7.14 (s, 1H), 6.94 (d, J = 8.5 Hz, 2H), 4.02 (s, 2H), 1.36 (s, 9H), 0.75 (d, J = 15.7 Hz, 4H).

33d was obtained according to the similar procedure of preparing **19a** using **15** and **32d**. White solid; yield 55%; ^{1}H NMR (300 MHz, $CDCl_3$) δ 8.54 (s, 1H), 8.41 (d, J = 9.0 Hz, 1H), 8.16 (d, J = 5.7 Hz, 1H), 8.03 (s, 1H), 7.84 (t, J = 8.4 Hz, 3H), 7.57 (s, 2H), 7.47 (t, J = 7.4 Hz, 1H), 7.35 (d, J = 9.1 Hz, 1H), 6.95 (d, J = 8.4 Hz, 2H), 6.67 (d, J = 5.4 Hz, 1H), 6.10 (s, 1H), 3.89 (s, 2H), 3.10 (d, J = 4.6 Hz, 3H), 0.77 (s, 2H), 0.65 (s, 2H). ^{13}C NMR (126 MHz, $CDCl_3$) δ 170.20, 166.53, 165.34, 162.52, 153.66, 152.34, 149.33, 134.92, 130.19, 129.32, 128.47, 128.08, 126.44, 125.95, 124.69, 121.65, 117.75, 114.73, 109.30, 102.61, 76.65, 27.02, 13.01. MS (ESI) m/z 483.20 $[M + H]^+$. HRMS: calcd for $C_{28}H_{27}N_4O_4$ $[M + H]^+$, 483.2027; found 483.2036.

5.2. Molecular docking

Docking study was performed using Maestro 9.3. X-ray crystal structure of FGFR1 (PDB ID: 4RWL) was downloaded from RCSB Protein Date Bank and prepared by Protein Preparation Wizard Workflow in the schrödinger program suite. Compound **25a** was prepared by Ligand Preparation and docked into the defined binding site without constraint. Based on the Glide-score, top ranking compounds were submitted. The final result for molecular docking was visualized by using PyMol.

5.3. ELISA kinase assay

The effects of indicated compounds on the activities of various tyrosine kinases were determined using enzyme-linked immunosorbent assays (ELISAs) with purified recombinant proteins. Briefly, 20 μg/mL poly (Glu, Tyr) $_{4:1}$ (Sigma, St Louis, MO, USA) was precoated in 96-well plates as a substrate. A 50-μL aliquot of 10 μM ATP solution diluted in kinase reaction buffer (50 mM HEPES [pH 7.4], 50 mM $MgCl_2$, 0.5 mM $MnCl_2$, 0.2 mM Na_3VO_4, and 1 mM DTT) was added to each well; 1 μL of various concentrations of indicated compounds diluted in 1% DMSO (v/v) (Sigma, St Louis, MO, USA) were then added to each reaction well. 1% DMSO (v/v) was used as the negative control. The kinase reaction was initiated by the addition of purified tyrosine kinase proteins diluted in 49 μL of kinase reaction buffer. After incubation for 60 min at 37 °C, the plate was washed three times with phosphate-buffered saline (PBS) containing 0.1% Tween 20 (T-PBS). Anti-phosphotyrosine (PY99) antibody (100 μL; 1:500, diluted in 5 mg/mL BSA T-PBS) was then added. After a 30-min incubation at 37 °C, the plate was washed three times, and 100 μL horseradish peroxidase-conjugated goat anti-mouse IgG (1:1000, diluted in 5 mg/mL BSA T-PBS) was added. The plate was then incubated at 37 °C for 30 min and washed 3 times. A 100-μL aliquot of a solution containing 0.03% H_2O_2 and 2 mg/mL o-phenylenediamine in 0.1 M citrate buffer (pH 5.5) was added. The reaction was terminated by the addition of 50 μL of 2 M H_2SO_4 as the color changed, and the plate was analyzed using a multi-well spectrophotometer (SpectraMAX190, from Molecular Devices, Palo Alto, CA, USA) at 490 nm. The inhibition rate (%) was calculated using the following equation: [1-(A490/A490 control)] × 100%. The IC_{50} values were calculated from the inhibition curves in two separate experiments.

5.4. Cell proliferation assay

Human lung cancer cell line NCI-H1581, human acute myelogenous leukemia cell line KG-1, human gastric cancer cell line SNU-16 were purchased from American Type Culture Collection (ATCC, Manassas, VA, USA). Human bladder cancer cell line RT-112 and Mouse Pre-B cell line BaF3 were purchased from DSMZ-German collection of microorganisms and cell cultures. Human bladder cancer cell line UMUC-14 was purchased from European Collection of Cell Cultures (ECACC). All the cell lines were routinely maintained in media according to the suppliers' recommendations and authenticated via short tandem repeats analysis by Genesky Biopharma Technology (last tested in 2016).

Cells were seeded in 96-well cell culture plates. On the day when seeding, the cells were exposed to various concentrations of compounds and further cultured for 72 h at 37 °C. Cell proliferation was then determined using Cell Counts Kit-8 (CCK8) or the thiazolyl blue tetrazolium bromide (MTT, from Sigma-Aldrich, St. Louis, MO, USA) assay. The IC50 values were calculated by concentration-response curve fitting using the four-parameter method.

5.5. Pharmacokinetic parameters in rats

Compound **25a** was administrated to male Sprague-Dawley (SD) rats (n = 3) either as a solution of 1 mg/kg in EtOH/PEG300/NaCl (10/40/50, v/v/v) intravenously or as a suspension of 3 mg/kg in DMSO/0.5% HPMC (5/95, v/v) orally by gavage. Blood samples were collected at 0.25, 0.5, 1, 2, 4, 6, 8 and 24 h following oral dosing. The blood samples were placed on wet ice, and serum was collected after 2 centrifugation. Serum samples were frozen and stored at −20 °C. The serum samples were analyzed utilizing HPLC-coupled tandem mass spectrometry (LC-MS/MS). All animal experiments were performed according to the institutional ethical guidelines on animal care and approved by the Institute Animal Care and Use Committee at Shanghai Institute of *Materia Medica*.

5.6. In vivo antitumor activity assay

Female nude mice (4–6 weeks old) were housed and maintained under specific pathogen-free conditions. Animal procedures were performed according to institutional ethical guidelines of animal care. The tumor cells at a density of 5×10^6 in 200 μL were injected subcutaneously (s.c.) into the right flank of nude mice and then allowed to grow to 700–800 mm^3, which was defined as a well-developed tumor. Subsequently, the well-developed tumors were cut into 1-mm [3] fragments and transplanted s. c. into the right flank of nude mice using a trocar. When the tumor volume reached 100–150 mm^3, the mice were randomly assigned into a vehicle control group (n = 12) and treatment groups (n = 6 per group). The control groups were given vehicle alone, and the treatment groups received 25a at the indicated doses via oral administration once daily for 3 weeks. The sizes of the tumors were measured twice per week using a microcaliper. Tumor volume (TV) = (length × width [2])/2, and the individual relative tumor volume (RTV) was calculated as follows: $RTV = V_t/V_0$, where V_t is the volume on a particular day and V_0 is the volume at the beginning of the treatment. The RTV was shown on indicated days as the median RTV ± SEM indicated for groups of mice. Percent (%) inhibition (TGI) values were measured on the final day of study for the drug-treated mice compared with vehicle-treated mice and were calculated as $100 \times \{1 - [(V_{\text{Treated Final day}} - V_{\text{Treated Day 0}})/(V_{\text{Control Final day}} - V_{\text{Control Day 0}})]$.

All animal experiments were performed according to the institutional ethical guidelines on animal care and approved by the Institute Animal Care and Use Committee at Shanghai Institute of *Materia Medica* (2017-04-DJ-26).

5.7. Statistical analysis

Data from in vitro assays are presented as the mean ± SD, whereas data from in vivo efficacy evaluations are presented as the mean ± SE. Significance was determined by Student's t-test, and differences were considered statistically significant at $^{*}p < 0.05$, $^{**}p < 0.01$, $^{***}p < 0.001$.

Acknowledgement

This work was supported by grants from National Natural Science Foundation of China (81703327, 81773565, 81430080, 81773762). Supporting from the International Cooperative Program (GJHZ1622) and Key Program of the Frontier Science (160621) of the Chinese Academy of Sciences, the Shanghai Commission of Science and Technology (16XD1404600, 14431900400), the "Personalized Medicines – Molecular Signature-based Drug Discovery and Development", Strategic Priority Research Program of the Chinese Academy of Sciences (No. XDA12020000) are also highly appreciated.

Appendix A. Supplementary data

Supplementary data related to this article can be found at https://doi.org/10.1016/j.ejmech.2018.05.005.

References

[1] M. Touat, E. Ileana, S. Postel-Vinay, F. Andre, J.C. Soria, Targeting FGFR signaling in cancer, Clin. Canc. Res. 21 (2015) 2684–2694.
[2] E.P. Carter, A.E. Fearon, R.P. Grose, Careless talk costs lives: fibroblast growth

factor receptor signalling and the consequences of pathway malfunction, Trends Cell Biol. 25 (2015) 221–233.
[3] N. Turner, R. Grose, Fibroblast growth factor signalling: from development to cancer, Nat. Rev. Canc. 10 (2010) 116–129.
[4] F.C. Kelleher, H. O'Sullivan, E. Smyth, R. McDermott, A. Viterbo, Fibroblast growth factor receptors, developmental corruption and malignant disease, Carcinogenesis 34 (2013) 2198–2205.
[5] A.A. Belov, M. Mohammadi, Molecular mechanisms of fibroblast growth factor signaling in physiology and pathology, Cold Spring Harbor Perspect. Biol. 5 (2013) a015958/1–a015958/24.
[6] C. Laestander, W. Engström, Role of fibroblast growth factors in elicitation of cell responses, Cell Prolif 47 (2014) 3–11.
[7] M.V. Dieci, M. Arnedos, F. Andre, J.C. Soria, Fibroblast growth factor receptor inhibitors as a cancer treatment: from a biologic rationale to medical perspectives, Canc. Discov. 3 (2013) 264–279.
[8] I.S. Babina, N.C. Turner, Advances and challenges in targeting FGFR signalling in cancer, Nat. Rev. Canc. 17 (2017) 318–332.
[9] J. Weiss, M.L. Sos, D. Seidel, M. Peifer, T. Zander, J.M. Heuckmann, et al., Frequent and focal FGFR1 amplification associates with therapeutically tractable FGFR1 dependency in squamous cell lung cancer, Sci. Transl. Med. 2 (2010), 62ra93.
[10] M. Tomiguchi, Y. Yamamoto, M. Yamamoto-Ibusuki, L. GotoYamaguchi, Y. Fujiki, S. Fujiwara, A. Sueta, M. Hayashi, T. Takeshita, T. Inao, H. Iwase, FGFR1 protein expression is associated with prognosis in ER-positive/HER2-negative primary breast cancer, Canc. Sci. 107 (2016) 491–498.
[11] H. Shoji, Y. Yamada, N. Okita, A. Takashima, Y. Honma, S. Iwasa, K. Kato, T. Hamaguchi, Y. Shimada, Amplification of FGFR2 gene in patients with advanced gastric cancer receiving chemotherapy: prevalence and prognostic significance, Anticancer Res. 35 (2015) 5055–5061.
[12] Y. Neuzillet, B.W. van Rhijn, N.L. Prigoda, B. Bapat, L. Liu, P.J. Bostrom, N.E. Fleshner, B.L. Gallie, A.R. Zlotta, M.A. Jewett, T.H. van der Kwast, FGFR3 mutations, but not FGFR3 expression and FGFR3 copy-number variations, are associated with favourable non-muscle invasive bladder cancer, Virchows Arch. 465 (2014) 207–213.
[13] J.G. Taylor VI, A.T. Cheuk, P.S. Tsang, J.Y. Chung, Y.K. Song, K. Desai, Y. Yu, Q.R. Chen, K. Shah, V. Youngblood, J. Fang, S.Y. Kim, C. Yeung, L.J. Helman, A. Mendoza, V. Ngo, L.M. Staudt, J.S. Wei, C. Khanna, D. Catchpoole, S.J. Qualman, S.M. Hewitt, G. Merlino, S.J. Chanock, J. Khan, Identification of FGFR4-activating mutations in human rhabdomyosarcomas that promote metastasis in xenotransplanted models, J. Clin. Invest. 119 (2009) 3395–3407.
[14] C. Gauglhofer, J. Paur, W.C. Schrottmaier, B. Wingelhofer, D. Huber, I. Naegelen, C. Pirker, T. Mohr, C. Heinzle, K. Holzmann, B. Marian, R. Schulte-Hermann, W. Berger, G. Krupitza, M. Grusch, B. Grasl-Kraupp, Fibroblast growth factor receptor 4: a putative key driver for the aggressive phenotype of hepatocellular carcinoma, Carcinogenesis 35 (2014) 2331–2338.
[15] N. Brady, P. Chuntova, L.K. Bade, K.L. Schwertfeger, The FGF/FGFR axis as a therapeutic target in breast cancer, Expet Rev. Endocrinol. Metabol. 8 (2013) 391–402.
[16] Y. Zhao, A.A. Adjei, Targeting angiogenesis in cancer therapy: moving beyond vascular endothelial growth factor, Oncol. 20 (2015) 660–673.
[17] M. Katoh, FGFR inhibitors: effects on cancer cells, tumor microenvironment and whole-body homeostasis (Review), Int. J. Mol. Med. 38 (2016) 3–15.
[18] Y. Cao, R. Cao, E.M. Hedlund, R Regulation of tumor angiogenesis and metastasis by FGF and PDGF signaling pathways, J. Mol. Med. (Berl.) 86 (2008) 785–789.
[19] R. Cao, H. Ji, N. Feng, Y. Zhang, X. Yang, P. Andersson, Y. Sun, K. Tritsaris, A.J. Hansen, S. Dissing, Y. Cao, Collaborative interplay between FGF-2 and VEGF-C promotes lymphangiogenesis and metastasis, Proc. Natl. Acad. Sci. U.S.A. 109 (2012) 15894–15899.
[20] R. Giavazzi, B. Sennino, D. Coltrini, A. Garofalo, R. Dossi, R. Ronca, M.P. Tosatti, M. Presta, Distinct role of fibroblast growth factor-2 and vascular endothelial growth factor on tumor growth and angiogenesis, Am. J. Pathol. 163 (2003) 1913–1926.
[21] Y. Yamamoto, J. Matsui, T. Matsushima, H. Obaishi, K. Miyazaki, K. Nakamura, O. Tohyama, T. Semba, A. Yamaguchi, S.S. Hoshi, F. Mimura, T. Haneda, Y. Fukuda, J.I. Kamata, K. Takahashi, M. Matsukura, T. Wakabayashi, M. Asada, K.I. Nomoto, T. Watanabe, Z. Dezso, K. Yoshimatsu, Y. Funahashi, A. Tsuruoka, Lenvatinib, an angiogenesis inhibitor targeting VEGFR/FGFR, shows broad antitumor activity in human tumor xenograft models associated with microvessel density and pericyte coverage, Vasc. Cell 6 (2014) 18.
[22] N. Awasthi, S. Hinz, R.A. Brekken, M.A. Schwarz, R.E. Schwarz, Nintedanib, a triple angiokinase inhibitor, enhances cytotoxic therapy response in pancreatic cancer, Canc. Lett. 358 (2015) 59–66.
[23] S.T. Kim, H.L. Jang, S.J. Lee, J. Lee, Y.L. Choi, K.M. Kim, J. Cho, S.H. Park, Y.S. Park, H.Y. Lim, M. Yashiro, W.K. Kang, J.O. Park, Pazopanib, a novel multitargeted kinase inhibitor, shows potent in vitro antitumor activity in gastric cancer cell lines with FGFR2 amplification, Mol. Canc. Therapeut. 13 (2014) 2527–2536.
[24] A.N. Brooks, E. Kilgour, P.D. Smith, Molecular pathways: fibroblast growth factor signaling: a new therapeutic opportunity in cancer, Clin. Canc. Res. 18 (2012) 1855–1862.
[25] N. Turner, A. Pearson, R. Sharpe, M. Lambros, F. Geyer, M.A. Lopez-Garcia, R. Natrajan, C. Marchio, E. Iorns, A. Mackay, C. Gillett, A. Grigoriadis, A. Tutt, J.S. Reis-Filho, A. Ashworth, FGFR1 amplification drives endocrine therapy resistance and is a therapeutic target in breast cancer, Canc. Res. 70 (2010) 2085–2094.
[26] P.R. Gavine, L. Mooney, E. Kilgour, A.P. Thomas, K. AlKadhimi, S. Beck, C. Rooney, T. Coleman, D. Baker, M.J. Mellor, A.N. Brooks, T. Klinowska, AZD4547: an orally bioavailable, potent, and selective inhibitor of the fibroblast growth factor receptor tyrosine kinase family, Canc. Res. 72 (2012) 2045–2056.
[27] V. Guagnano, P. Furet, C. Spanka, V. Bordas, M. Le Douget, C. Stamm, J. Brueggen, M.R. Jensen, C. Schnell, H. Schmid, M. Wartmann, J. Berghausen, P. Drueckes, A. Zimmerlin, D. Bussiere, J. Murray, D. Graus Porta, Discovery of 3-(2,6-dichloro-3,5-dimethoxy-phenyl)-1-{6-[4-(4-ethyl-piperazin-1-yl)-phenylamino]-pyrimidin-4-yl}-1-methyl-urea (NVP-BGJ398), a potent and selective inhibitor of the fibroblast growth factor receptor family of receptor tyrosine kinase, J. Med. Chem. 54 (2011) 7066–7083.
[28] J. Zhang, L. Zhang, X. Su, M. Li, L. Xie, F. Malchers, S. Fan, X. Yin, Y. Xu, K. Liu, Z. Dong, G. Zhu, Z. Qian, L. Tang, J. Schöttle, P. Zhan, Q. Ji, E. Kilgour, P.D. Smith, A.N. Brooks, R.K. Thomas, P.R. Gavine, Translating the therapeutic potential of AZD4547 in FGFR1-amplified non-small cell lung cancer through the use of patient-derived tumor xenograft models, Clin. Canc. Res. 18 (2012) 6658–6667.
[29] L. Nogova, L.V. Sequist, J.M. Perez Garcia, F. Andre, J.P. Delord, M. Hidalgo, J.H. Schellens, P.A. Cassier, D.R. Camidge, M. Schuler, U. Vaishampayan, H. Burris, G.G. Tian, M. Campone, Z.A. Wainberg, W.T. Lim, P. LoRusso, G.I. Shapiro, K. Parker, X. Chen, S. Choudhury, F. Ringeisen, D. Graus-Porta, D. Porter, R. Isaacs, R. Buettner, J. Wolf, Evaluation of BGJ398, a fibroblast growth factor receptor 1-3 kinase inhibitor, in patients with advanced solid tumors harboring genetic alterations in fibroblast growth factor receptors: results of a global phase I, dose-escalation and dose-expansion study, J. Clin. Oncol. 35 (2017) 157–165.
[30] J. Taeger, C. Moser, C. Hellerbrand, M.E. Mycielska, G. Glockzin, H.J. Schlitt, E.K. Geissler, O. Stoeltzing, S.A. Lang, Targeting FGFR/PDGFR/VEGFR impairs tumor growth, angiogenesis, and metastasis by effects on tumor cells, endothelial cells, and pericytes in pancreatic cancer, Mol. Canc. Therapeut. 10 (2011) 2157–2167.
[31] R. Dienstmann, J. Rodon, A. Prat, J. Perez-Garcia, B. Adamo, E. Felip, J. Cortes, A.J. Iafrate, P. Nuciforo, J. Tabernero, Genomic aberrations in the FGFR pathway: opportunities for targeted therapies in solid tumors, Ann. Oncol. 25 (2014) 552–563.
[32] D. Li, K. Xie, L. Zhang, X. Yao, H. Li, Q. Xu, X. Wang, J. Jiang, J. Fang, Dual blockade of vascular endothelial growth factor (VEGF) and basic fibroblast growth factor (FGF-2) exhibits potent anti-angiogenic effects, Canc. Lett. 377 (2016) 164–173.
[33] E. Bello, G. Colella, V. Scarlato, P. Oliva, A. Berndt, G. Valbusa, S.C. Serra, M. D'Incalci, E. Cavalletti, R. Giavazzi, G. Damia, G. Camboni, E-3810 is a potent dual inhibitor of VEGFR and FGFR that exerts antitumor activity in multiple preclinical models, Cancer. Res. 71 (2011) 1396–1405.
[34] C.D. Sohl, M.R. Ryan, B. Luo, K.M. Frey, K.S. Anderson, Illuminating the molecular mechanisms of tyrosine kinase inhibitor resistance for the FGFR1 gatekeeper mutation: the Achilles' heel of targeted therapy, ACS Chem. Biol. 10 (2015) 1319–1329.
[35] X.F. Jiang, Y. Dai, X. Peng, Y.Y. Shen, Y. Su, M.M. Wei, W.R. Liu, Z.B. Ding, A. Zhang, Y.H. Shi, J. Ai. SOMCL-085, a novel multi-targeted FGFR inhibitor, displays potent anticancer activity in FGFR-addicted human cancer models. Acta Pharmacol. Sin. DOI: 10.1038/aps.2017.96.
[36] M.S. Watanabe, Y. Yamamoto, K. Kodama, Y. Miyajima, M. Mikamoto, T. Nakagawa, H. Kuramochi, S. Funasaka, S. Nagao, N.H. Sugi, K. Okamoto, Y. Minoshima, Y. Nakatani, Y. Karoji, I. Ohashi, Y. Yamane, T. Okada, T. Matsushima, J. Matsui, M. Iwata, T. Uenaka, A. Tsuruoka, E7090, a novel selective inhibitor of fibroblast growth factor receptors, displays potent antitumor activity and prolongs survival in preclinical models, Mol. Canc. Therapeut. 15 (2016) 2630–2639.
[37] J.C. Harmange, M.M. Weiss, J. Germain, A.J. Polverino, G. Borg, J. Bready, D. Chen, D. Choquette, A. Coxon, T. DeMelfi, L. DiPietro, N. Doerr, J. Estrada, J. Flynn, R.F. Graceffa, S.P. Harriman, S. Kaufman, D.S. La, A. Long, M.W. Martin, S. Neervannan, V.F. Patel, M. Potashman, K. Regal, P.M. Roveto, M.L. Schrag, C. Starnes, A. Tasker, Y. Teffera, L. Wang, R.D. White, D.A. Whittington, R. Zanon, Naphthamides as novel and potent vascular endothelial growth factor receptor tyrosine kinase inhibitors: design, synthesis, and evaluation, J. Med. Chem. 51 (2008) 1649–1667.
[38] W.A. Kinney, M.E. McDonnell, H.M. Zhong, C. Liu, L. Yang, W. Ling, T. Qian, Y. Chen, Z. Cai, D. Petkanas, D.E. Brenneman, Discovery of KLS-13019, a cannabidiol-derived neuroprotective agent, with improved potency, safety, and permeability, ACS Med. Chem. Lett. 7 (2016) 424–428.
[39] G.A. Kraus, Y. Zeng, A synthetic equivalent of 3,5-dimethoxyphenyl lithium. A facile route to 5-substituted resorcinols, Synth. Commun. 30 (2000) 2133–2141.
[40] Y. Wang, Z. Chen, M. Dai, P. Sun, C. Wang, Y. Gao, H. Zhao, W. Zeng, L. Shen, W. Mao, T. Wang, G. Hu, J. Li, S. Chen, C. Long, X. Chen, J. Liu, Y. Zhang, Discovery and optimization of selective FGFR4 inhibitors via scaffold hopping, Bioorg. Med. Chem. Lett 27 (2017) 2420–2423.
[41] S.H. Chen, Z.X. Chen, M.B. Dai, C. Xie, P. Li, Y. Zhang, G.B. Liang, Q. Wang, J.P. Liao, F. Sun, G.P. Hu, J. Li, Preparation of vinyl compounds as FGFR and VEGFR inhibitors, PCT Int. Appl (August 3, 2016). WO 2017024968 A1.
[42] J.M. Cox, H.D. Chu, M.V. Chelliah, J.S. Debenham, K. Eagen, P. Lan, M. Lombardo, C. London, M.A. Plotkin, U. Shah, Z. Sun, H.M. Vaccaro, S. Venkatraman, T. Suzuki, N. Wang, E.R. Ashley, A. Crespo, M. Madeira, D.H. Leung, C. Alleyne, A.M. Ogawa, S. Souza, B. Thomas-Fowlkes, J. Di Salvo,

A. Weinglass, M. Kirkland, M. Pachanski, M.A. Powles, E. Tozzo, T.E. Akiyama, F. Ujjainwalla, J.R. Tata, C.J. Sinz, Design, synthesis, and evaluation of novel and selective G-protein coupled receptor 120 (GPR120) spirocyclic agonists, ACS Med. Chem. Lett. 8 (2016) 49–54.

[43] Y. Charton, C. Guillonneau, B. Lockhart, P. Lestage, S. Goldstein, Preparation and affinity profile of novel nicotinic ligands, Bioorg. Med. Chem. Lett 18 (2008) 2188–2193.

[44] V. Gore, S. Gravel, C. Cossette, P. Patel, S. Chourey, Q.j Ye, J. Rokach, W.S. Powell, Inhibition of 5-oxo-6,8,11,14-eicosatetraenoic acid-induced activation of neutrophils and eosinophils by novel indole OXE receptor antagonists, J. Med. Chem. 57 (2014) 364–377.